

5-1-2011

## Multi-objective design optimization framework for structural health monitoring

Danny Loren Parker

Follow this and additional works at: <https://scholarsjunction.msstate.edu/td>

---

### Recommended Citation

Parker, Danny Loren, "Multi-objective design optimization framework for structural health monitoring" (2011). *Theses and Dissertations*. 3231.  
<https://scholarsjunction.msstate.edu/td/3231>

This Dissertation - Open Access is brought to you for free and open access by the Theses and Dissertations at Scholars Junction. It has been accepted for inclusion in Theses and Dissertations by an authorized administrator of Scholars Junction. For more information, please contact [scholcomm@msstate.libanswers.com](mailto:scholcomm@msstate.libanswers.com).

MULTI-OBJECTIVE DESIGN OPTIMIZATION FRAMEWORK FOR  
STRUCTURAL HEALTH MONITORING

By

Danny Loren Parker

A Dissertation  
Submitted to the Faculty of  
Mississippi State University  
in Partial Fulfillment of the Requirements  
for the Degree of Doctor of Philosophy  
in Electrical Engineering  
in the Department of Electrical and Computer Engineering

Mississippi State, Mississippi

April 2011

Copyright by  
Danny Loren Parker  
2011

MULTI-OBJECTIVE DESIGN OPTIMIZATION FRAMEWORK FOR  
STRUCTURAL HEALTH MONITORING

By

Danny Loren Parker

Approved:

---

Nicolas H. Younan  
Professor of Electrical and Computer  
Engineering, and Department Head  
(Major Professor and Dissertation Di-  
rector)

---

Randolph F. Follett  
Assistant Professor of Electrical and  
Computer Engineering  
(Committee Member)

---

Jenny Q. Du  
Associate Professor of Electrical  
and Computer Engineering  
(Committee Member)

---

James E. Fowler  
Professor of Electrical  
and Computer Engineering,  
and Graduate Coordinator

---

Wm. Garth Frazier  
Graduate Committee Participant  
(Committee Member)

---

Sarah A. Rajala  
Dean of the James Worth Bagley  
College of Engineering

Name: Danny Loren Parker

Date of Degree: April 29, 2011

Institution: Mississippi State University

Major Field: Electrical Engineering

Major Professor: Dr. Nicolas Younan

Title of Study: MULTI-OBJECTIVE DESIGN OPTIMIZATION FRAMEWORK  
FOR STRUCTURAL HEALTH MONITORING

Pages in Study: 79

Candidate for Degree of Doctor of Philosophy

The purpose of this dissertation is to demonstrate the ability to design health monitoring systems from a systematic perspective and how, with proper sensor and actuator placement, damage occurring in a structure can be detected and tracked. To this end, a design optimization was performed to determine the best locations to excite the structure and to collect data while using the minimum number of sensors. The type of sensors used in this design optimization was uni-axis accelerometers. It should be noted that the design techniques presented here are not limited to accelerometers. Instead, they allow for any type of sensor (thermal, strain, electromagnetic, etc.) and will find the optimal locations with respect to defined objective functions (sensitivity, cost, etc.). The use of model-based optimization techniques for the design of the monitoring system is driven by the desire to obtain the best performance possible from the system given what is known about the system prior to implementation. The use of a model is more systematic than human judgment

and is able to take far more into account by using information about the dynamical response of a system than even an experienced structural engineer. It is understood in the context of structural modeling that no model is 100% accurate and that any designs produced using model-based techniques should be tolerant to modeling errors. Demonstrations performed in the past have shown that poorly placed sensors can be very insensitive to damage development.

To perform the optimization, a multi-objective genetic algorithm (GA) was employed. The objectives of the optimization were to be highly sensitive to damage occurring in potential ‘hot spots’ while also maintaining the ability to detect damage occurring elsewhere in the structure and maintaining robustness to modeling errors. Two other objectives were to minimize the number of sensors and actuators used. The optimization only considered placing accelerometers, but it could have considered different type of sensors (i.e. strain, magneto-restrictive) or any combination thereof.

Key words: Optimization, Structural Health Monitoring, Genetic Algorithm, Health Monitoring Design,

## DEDICATION

To my Son and Daughter whom I love very much.

## ACKNOWLEDGMENTS

It is often said that no work is done in a vacuum and this effort was no exception. There are many people whose support and assistance played an important role in the realization of this dissertation. To begin with, I'd like to thank Dr. W. Garth Frazier for his guidance and assistance over the years; he has been an invaluable resource and friend through the many years of effort to bring a design philosophy to the field of structural health monitoring. I'd also like to thank my colleagues, especially Pam McCulley, Josh Cassity, and Matt Jones, for all their help over the years; their efforts in running code, setting up experiments, and collecting data all the while plagued by every imaginable complication have allowed this work to move beyond theory and into reality.

In addition, I'd like to acknowledge both the Air Force Research Lab at Wright Patterson and the Army Diagnostics and Prognostics labs for their support. Over the years, they have generously provided parts for experimentation, lab space, and, most importantly, an insight into the issues and needs that drive the push to incorporate health monitoring into their fleets. The technology has benefited immensely from their cooperation and support.

I thank my committee for their thoughtful comments and the time they devoted on this dissertation. I also thank Dr. Nicolas Younan for directing this research and



guiding this document, without which, this document would not be anywhere near the quality it is.

Lastly, I thank my family for supporting me during this period of my life. There were many weeks and months they barely saw me between working a job all day and then classes all night. Without my kids' understanding and the unending support of my wife, Janette, in allowing me the time and creating the opportunity, this dissertation would have never come to fruition.

## TABLE OF CONTENTS

DEDICATION . . . . .	ii
ACKNOWLEDGMENTS . . . . .	iii
LIST OF TABLES . . . . .	vii
LIST OF FIGURES . . . . .	viii
LIST OF SYMBOLS, ABBREVIATIONS, AND NOMENCLATURE . . . . .	x
CHAPTER	
1. INTRODUCTION . . . . .	1
1.1 Background . . . . .	1
1.2 Motivation . . . . .	4
1.3 Contributions . . . . .	5
2. LITERATURE REVIEW . . . . .	7
3. METHODOLOGY . . . . .	9
3.1 Multi-Objective Optimization . . . . .	11
3.1.1 Weighted Sum Method . . . . .	12
3.1.2 Pareto Optimal Solution . . . . .	12
3.1.2.1 Definition of a Pareto Surface . . . . .	14
3.2 Objective Functions . . . . .	14
3.2.1 Sensitivity . . . . .	15
3.2.1.1 Known likely damage areas . . . . .	16
3.2.1.2 Global Sensitivity . . . . .	18
3.2.2 Minimum Number of Sensors . . . . .	21
3.2.3 Robustness . . . . .	21
3.3 Genetic Algorithm . . . . .	22

3.3.1	Finding the Pareto Surface in the Context of a Genetic Algorithm . . . . .	24
4.	RESULTS . . . . .	28
4.1	Model . . . . .	29
4.1.1	Model Refinement . . . . .	31
4.2	Design Surface . . . . .	32
4.2.1	Design Results . . . . .	33
4.2.2	Evaluating Design Optimality via Exhaustive Search . . . . .	37
4.2.3	Evaluating Design Robustness . . . . .	41
4.2.3.1	Evaluating the Design Sensitivity Numerically . . . . .	42
4.2.3.2	Monte Carlo Evaluations of Design Sensitivity . . . . .	45
4.3	Simulated Results . . . . .	52
4.3.1	Simulated Damage Detection . . . . .	52
4.3.1.1	Detector Design . . . . .	55
4.4	Experimental Results . . . . .	59
5.	CONCLUSIONS . . . . .	69
5.1	Summary of Work . . . . .	69
5.2	Recommendation for Continued Research . . . . .	73
	BIBLIOGRAPHY . . . . .	76

## LIST OF TABLES

4.1	Crack Size & Health Monitoring System Run Numbers . . . . .	64
4.2	Confusion Matrix for Statistical Damage Detector . . . . .	68

## LIST OF FIGURES

4.1	Landing Gear Designs . . . . .	35
4.2	Roof Strap Designs . . . . .	36
4.3	Surrogate Rainbow Fitting Design . . . . .	38
4.4	Simple Cantilever Beam Model . . . . .	39
4.5	Contour Plot of $dQ_y$ . . . . .	41
4.6	Histogram of Model Density . . . . .	47
4.7	Histogram of Sensitivities . . . . .	48
4.8	Sensitivity vs. Density . . . . .	49
4.9	Sensitivity vs. Modulus . . . . .	51
4.10	Simulated Response of Roof Strap . . . . .	56
4.11	Simulated Response of Landing Gear . . . . .	57
4.12	Landing Gear Experimental Setup . . . . .	60
4.13	Landing Gear Results: Optimal (Blue) Human (Red) . . . . .	61
4.14	Roof Strap Experimental Setup . . . . .	63
4.15	Bolt Loosening Results: Optimal (Blue) Human (Red) . . . . .	64
4.16	Roof Strap Cut Results: Optimal (Blue) Human (Red) . . . . .	65
4.17	Cut at Completion of Test . . . . .	66
4.18	Damage Metric vs. Sample Number with Crack Size Overlaid . . . . .	67

4.19 Z-Test Result at 99.999999% Confidence; Crack Size Overlaid . . . . .	68
--	----

## LIST OF SYMBOLS, ABBREVIATIONS, AND NOMENCLATURE

<b>NDI</b>	Non-Destructive Inspection
<b>SHM</b>	Structural Health Monitoring
<b>NDI/E</b>	Non-Destructive Inspection and Evaluation
<b>RUL</b>	Remaining Useful Life
<b>CBM</b>	Condition-Based Maintenance
<b>IVHM</b>	Integrated Vehicle Health
<b>MOGA</b>	Multi-Objective Genetic Algorithm
<b>GA</b>	Genetic Algorithm
<b>DOF</b>	Degrees of Freedom
<b>MOO</b>	Multi-Objective Optimization
<b>SUS</b>	Stochastic Universal Sampling
<b>FE</b>	Finite-Element
<b>FD</b>	Finite-Difference
<b>FDTD</b>	Finite-Difference Time-Domain
<b>FEM</b>	Finite-Element Model
<b>DMS</b>	Damage Monitoring System
<b>DAQ</b>	Data Acquisition
<b>SNR</b>	Signal-to-Noise

# CHAPTER 1

## INTRODUCTION

### 1.1 Background

Aging of vehicles (airplanes, helicopters, etc.) and civil infrastructure (buildings, bridges, etc.) is a complex process that typically involves a slowly evolving degradation. Because the factors affecting the integrity and functionality of these structures are too complex and chaotic to be more than guessed at, the processes driving the degradation must be periodically monitored in some manner [2]. Today, the most common form of assessing the condition of a structure is through non-destructive inspection (NDI) methods such as ultrasonic, eddy current, or even visual inspections [5]. This approach is limited because inspection interval have to be set based upon amount of usage, which is typically very conservative in order to keep the risk manageable and is often loosely correlated with the actual damage state of the part.

Structural Health Monitoring (SHM) could provide more quantitative data on the integrity and condition of the monitored structure [36]. It is based on the use of multisensor systems for the monitoring of parameters that are important for the functionality and safety of monitored structures [24]. Collection of the appropriate measurements over time, along with proper data analysis, can not only lead to the prevention of critical failures, but can also provide much more efficient use of mainte-



nance resources. One of the key stumbling blocks to fielding these systems is finding out which of these measurements are necessary, and then how to collect them with minimal cost.

SHM is a relatively new field that has mainly grown out of the non-destructive inspection and evaluation (NDI/E) discipline. SHM's main focus is assessing the damage of the structural underpinning of infrastructure (buildings, bridges, aircrafts, etc.) using systems integrated into the structure being monitored. Damage can include things such as cracking, corrosion, and fatigue. By and large, those practicing SHM concern themselves with four main problem subcategories as laid out by [35]:

1. The detection of damage within a structure;
2. The localization of damage within a structure;
3. The characterization of the type of damage; and
4. The ability to predict the remaining useful life (RUL) given some expected operating conditions.

The ability to accurately and dependably assess the health of a structure can provide important information on matters as diverse as effective safety-testing of a structure after some major event (earthquake, explosion, etc.), as well as condition-based maintenance (CBM) [4]. CBM is a major push for maintainers of vehicle systems because structural maintenance significantly impacts sustainment costs and operational availability of rotorcraft. Manual airframe inspections can be time-consuming and the results can be unreliable [32]. Fixed, fleet-wide retirement lives provide an acceptable level of risk, but can also result in required maintenance at inopportune times, adversely affecting availability; in addition, they do not support risk-based

decisions with respect to operational status [17]. Battle damage can also result in additional aircraft downtime for assessment and repair design. In order to make better maintenance decisions that minimize risk and cost, operators need a robust inspection system linked to analysis tools so that structural integrity can be assessed quickly, as well as operational limitations and remaining useful life determined to allow informed, risk-based decisions on maintenance and operational status of each aircraft [26].

CBM has been driven by the maintainer's demand to increase system efficiency through elimination of unnecessary maintenance in a system. A CBM system's goal is to determine the equipment's health and alert the maintainers only when maintenance is actually necessary [21]. Ideally, CBM will allow the maintenance personnel to do only the necessary maintenance, thus minimizing spare parts cost, system downtime, and overall time spent on maintenance. This approach to maintenance relies on monitoring the condition of a system in order to detect anomalies, as well as the ability to accurately and effectively diagnose the health of critical components. One of the key enablers for CBM is on-board systems that can monitor system parameters to allow for the damage condition to be assessed. To this end, the use of integrated vehicle health monitoring (IVHM) systems in CBM continues to become more prevalent, especially with respect to electronic subsystems and rotating mechanical components. Conversely, widespread integrated health monitoring of structural components does not exist for several reasons, including the lack of a

systematic methodology for designing these complex systems [11]. This lack of design methodology is what is addressed in this dissertation.

## 1.2 Motivation

As noted by Doebling, et al. [11], one of the main factors currently preventing widespread and universal adoption of SHM technologies is the lack of a systematic design method. A good design methodology should :

- have the ability to select from and place different types of sensors;
- have the ability to select from and place different types of actuators;
- be designed to maximize the ability to detect, localize, and characterize damage;
- be robust to variations due to modeling or manufacturing error; and
- be equally applicable to both legacy (known issues) and future vehicles (unknown issues).

It is the intent of this study to suggest such a methodology for structural health monitoring using parametric models, formal mathematical metrics for design evaluation, and multi-objective optimization concepts. The use of model-based optimization techniques for the design of the monitoring system is driven by the desire to obtain the best performance possible from the system, given what is known about the system prior to implementation. The use of a model is far more systematic than human judgment and is able to take far more into account concerning the dynamical response of a system than even an experienced structural engineer. In the context of structural modeling, it is understood that no model ever achieves 100% accuracy and that any designs produced using model-based techniques should be tolerant to

modeling errors. In the optimization, the allowable sensor-actuator locations can be defined so that the resulting designs are easier to manufacture. The result of a design is a set of sensor-actuator locations.

### 1.3 Contributions

The immediate and clear contributions of this research are the ability to design health monitoring systems from a systematic perspective and how with proper sensor and actuator placement damage occurring in a structure can be detected. To this end, a design optimization was performed to determine the best locations to excite the structure and to collect data while using the minimum number of sensors, since system weight is an important factor in any aerospace application. Other contributions include the development of novel objective functions for:

- optimizing sensor and actuator positions and type for detecting damage in expected locations (hotspots);
- optimizing sensor and actuator positions and type for detecting damage globally; and
- being robust to modeling error and manufacturing variations.

The framework for selecting sensor and actuator locations according to a procedure that optimizes the ability to detect change in the structure's dynamics with respect to the chosen detection algorithm is done using a multi-objective genetic algorithm (MOGA) that produces a Pareto set of designs. That is, the choice of where to place sensors and actuators is tied closely to the signal-processing algorithm (detector) being employed. It has been shown [14] that optimal sensor positioning for

estimating the parameters characterizing damage is not necessarily the same as the optimal positioning for detection. This should not be a surprise to those readers who are familiar with electronic communications systems where it is well-known that the solution (matched filter) to the optimal yes-no detection problem is not the same as the optimal least-squares signal estimator (Wiener filter) problem.

It should be noted that the design techniques presented here are not limited to one single type of sensor. Instead, the techniques allow for any type of sensor (thermal, strain, electromagnetic, etc.) and will maximize the optimal locations with respect to defined objective functions (sensitivity, cost, etc.).

## CHAPTER 2

### LITERATURE REVIEW

Using multi-objective optimization (MOO) for design is not a new concept; in fact, it has been used successfully in a number of fields other than health monitoring. Examples of work done using optimization for design are too numerous to cite in full, but many examples are listed in standard textbooks on the subject, such as [3, 12, 16]. In the field of structures, [38], [19], and [23] have developed methods for selection of noisy actuator and sensor locations on flexible aerospace structures for modal identification or shape control. In most methods, however, the selection of sensor types and their locations on the structure are chosen based on intuition and engineering judgment; however, the use of design optimization techniques is becoming more common. Most current sensor placement methodologies are focused on maximizing the controllability and observability of the healthy structure and usually only focus on minimizing the number of sensors and one additional objective. In [6], the author's objective was the optimal placement of sensors and actuators for controllability and observability. This was accomplished by examining the whole structure and selecting sensor locations to maximize the signal-to-noise ratio in the system. Other approaches examine ways to minimize the information entropy norm, which measures the uncertainty for parameter estimating [42] by selecting a number

of damageable areas and placing an equal number of sensors to minimize the uncertainty in parameter estimates. There are many such techniques—all with different objective function for modal and parametric identification in structures—but very few that are specific for damage detection.

For damage detection in particular, [7] discusses a method using a sensitivity analysis to find the degrees of freedom that maximizes the changes due to damage in the observable eigenstructure. [37, 18, 28] exploit properties of the Fischer information matrix to find the optimal sensor placement with respect to damage. The previous techniques focus on sensor placement and typically lack any optimization for actuator locations. [25] used a simple static Tabu Search method to seek the number and location of sensors. The genetic algorithm (GA) is particularly effective at finding optimal solutions that are widely scattered throughout the design space. Using a GA and a finite element analysis technique, [39] developed an optimal sensor placement procedure that is used to determine the optimal sensor pattern for detecting seeded delaminations located anywhere in a composite plate. The work presented in reference [31] is very close in spirit to the work presented herein. This work is in many respects a continuation of the work started in collaboration with Rinehart documented in [33].

CHAPTER 3  
METHODOLOGY

We begin our discussion by reviewing the essential elements of linear, finite-dimensional, time-invariant (LTI) dynamical systems theory [1, 22] that are needed to develop our approach. This is followed by the presentation of an example application to a prototypical wing spar structure. Assume that the physical phenomena (elastic, thermal, electromagnetic, etc.) of interest for the structure can be modeled adequately as a LTI dynamical system in state-space form ([30]); i.e.,

$$\begin{aligned}\dot{x}(t) &= Ax(t) + Bu(t) \\ y(t) &= Cx(t) + Du(t) \\ x(0) &= x_o\end{aligned}\tag{3.1}$$

where  $x(t) \in \mathbb{R}^n$  is the state vector,  $u(t) \in \mathbb{R}^m$  is the actuator signal vector,  $y(t) \in \mathbb{R}^p$  is the sensor signal vector, and  $x_o \in \mathbb{R}^n$  is the initial state condition. The matrices  $A \in \mathbb{R}^{n \times n}$ ,  $B \in \mathbb{R}^{n \times m}$ ,  $C \in \mathbb{R}^{p \times n}$ , and  $D \in \mathbb{R}^{p \times p}$  represent the system dynamics, actuator influence, sensor coupling, and direct feed through effects, respectively. Here, the symbols  $\mathbb{R}^n$  and  $\mathbb{R}^{n \times m}$  are used to represent the spaces of  $n$ -dimensional real vectors and  $n$ -by- $m$  real matrices, respectively. While this model framework may seem restrictive at first, it should be recalled that linear elastic finite-element



methods (FEM) and finite-difference (FD) heat transfer modeling can be represented by this form quite easily.

To highlight a particular case, consider the familiar second-order vector form resulting from the application of FEM to an elastic structure:

$$M\ddot{z}(t) + G\dot{z}(t) + Kz(t) = Fu(t) \quad (3.2)$$

where  $M$ ,  $G$ , and  $K$  are the mass, damping, and stiffness matrices, respectively. Here, the matrix  $F$  maps the actuator signals into the usual force vector and should be thought of as specifying where independent forces are applied to the structure. The vector  $z$  consists of the translational and rotational degrees-of-freedom (DOF). Using the definition

$$x(t) = \begin{bmatrix} z(t) \\ \dot{z}(t) \end{bmatrix} \quad (3.3)$$

Equation 3.2 can be rearranged into the standard state space form shown in 3.1, where

$$A = \begin{bmatrix} 0 & I \\ -M^{-1}K & -M^{-1}G \end{bmatrix} \quad (3.4)$$

$$B = \begin{bmatrix} 0 \\ M^{-1}F \end{bmatrix}$$

The definitions of  $C$  and  $D$  are dependent on the type of sensor chosen. For the case of an accelerometer, which will be the example sensor throughout this paper,

$$y(t) = C_a \ddot{z}(t) \quad (3.5)$$

and, from a rearrangement of equation 3.2 and a substitution of 3.3, it can be shown that

$$\ddot{z}(t) = M^{-1}(Fu(t) - Gx_2(t) - Kx_1(t)) \quad (3.6)$$

substituting 3.6 into 3.5 and multiplying through yields

$$y(t) = -C_a M^{-1} \begin{bmatrix} K & G \end{bmatrix} x(t) + C_a M^{-1} Fu(t) \quad (3.7)$$

where  $C_a$  is a matrix specifying the locations of the accelerometers. To fully express the system in the form defined by 3.1, it necessitates that  $C = C_a M^{-1} \begin{bmatrix} K & G \end{bmatrix}$  and  $D = C_a M^{-1} F$ . The structure of the matrix  $C_a$  is such that each row corresponds to the output of an accelerometer and each column corresponds to a DOF in the model. A value for the accelerometer's sensitivity to acceleration is placed in the column corresponding to the DOF being measured. Note that no row can have more than a single non-zero value. All other entries in a row should be zero. This sensor model can be further enhanced to include the sensor's bandwidth and the overall transfer function.

### 3.1 Multi-Objective Optimization

Multi-Objective Optimization (MOO) is an optimization method that competes multiple cost functions to find the best tradeoffs. In multi-objective optimization,

there is not one single best solution, but instead a possibly infinite number of optimal solutions that lie on the Pareto Frontier. For example, there is a trade-off between driving fast and getting good gas mileage and, once the optimal solutions are found, one needs to pick the best tradeoff for the current situation.

### 3.1.1 Weighted Sum Method

Weighted sum is a method that reduces the results of multiple objective functions into a single objective function. It does so by assigning a weight to each objective function and then sums the results to a scalar value representing the “goodness” of the solution [43]. This allows the use of traditional gradient-based methods, which are restricted to single-objective optimizations, to attempt to solve MOO tasks. One drawback to this method is that the weights are typically chosen *a priori* based on the objective function’s perceived importance to the designer. This presupposition limits the possible solutions to only the ones on the lying on the manifold defined by the weights.

### 3.1.2 Pareto Optimal Solution

One method that alleviates the designer from having to make *a priori* judgments about the importance of particular objectives is to try to find the Pareto optimal solution. The Pareto optimal solution is one where, in order to improve a single criterion, other criteria must be degraded in performance. The term is named after Vilfredo Pareto, an Italian economist who used the concept in his studies of economic

efficiency and income distribution [29]. The Pareto solution or Pareto surface, as it is sometimes called, is the mathematical embodiment of all possible optimal solutions. Thus, in the most general sense, the mathematics of optimization focuses on finding solutions close to this Pareto surface.

Pareto optimality is an important concept originally defined in economics, [20], but is now additionally applied to engineering as well as in game theory and social sciences [40]. Given a set of criterion, improving performance of one criterion that does not reduce another criteria is called a Pareto improvement. An allocation or design is Pareto optimal when no further Pareto improvements can be made.

The Pareto frontier or Pareto surface is the set of solutions that are all Pareto optimal – that no individual parameter can be improved without another parameter being made worse [8]. Finding Pareto frontiers is particularly useful in engineering. By calculating a range of potentially optimal solutions, a designer can make focused trade-offs within this constrained set of parameters, rather than needing to consider the full ranges of parameters. The idea of finding system designs that lie on the Pareto surface will be used in evaluating the optimal designs in this effort.

Each axis of the Pareto surface represents one of the objectives of the optimization. When there are more than three simultaneous objectives it becomes difficult to visualize the resulting trade-off, and so data visualization techniques are required. By definition, the end point on one axis of the Pareto surface is the equivalent of doing a single objective optimization on just that dimension.

### 3.1.2.1 Definition of a Pareto Surface

Assume that the design criteria for a particular problem is dependent on  $n$  different objectives that may or may not be dependent on each other and is represented by the set of functions

$$f : \mathfrak{R}^n \rightarrow \mathfrak{R}^m \tag{3.8}$$

where the set  $X$  represents all possible solutions to the problem in the metric space  $\mathfrak{R}^n$ , and  $Y$  represents all possible objective vectors in  $\mathfrak{R}^m$  such that

$$Y = \{y \in \mathfrak{R}^m : y = f(x), x \in X\} \tag{3.9}$$

Assuming that our goal is to maximize the objectives, an objective vector  $y'' \in \mathfrak{R}^m$  is referred to as strictly dominating another point  $y' \in \mathfrak{R}^m$  when  $y'' \succ y'$ , where

$$y'' \succ y' \rightarrow \{y''_i > y'_i : i \in \{1, 2, \dots, m\}, y'' \neq y'\} \neq \emptyset \tag{3.10}$$

The Pareto surface is thus defined as

$$P(Y) = \{y' \in Y : \{y'' \in Y : y'' \succ y', y'' \neq y'\} = \emptyset\} \tag{3.11}$$

## 3.2 Objective Functions

Objective functions are a statement about what makes a particular solution better or worse than another. They are typically easy to qualify as in “I want a design

that is high performance”; but they are often hard to quantify formally. What is meant by “high performance?” In general, objective functions are the mathematical embodiment of what a designer hopes to accomplish. Teasing out and properly quantifying this information from various stakeholders is typically where the art is in any optimization problem.

This section will discuss the objective (or cost) function that will be used in evaluating a particular design’s performance with respect to monitoring the health of a structure. As laid out earlier, it is important for structural health monitoring systems to be maximally sensitive to damage developing in areas of high likelihood of damage, while also ensuring there are no places damage will be missed. The system will also be required to be robust to errors in the model used for the optimization, while having a minimal number of sensors to keep the weight and cost low.

### **3.2.1 Sensitivity**

The sensitivity of a design to damage is of the utmost importance in health monitoring systems. There are many different ways to define sensitivity but for the purposes of this work, it is defined as a change in the output signal (typically voltages being monitored) due to changes in the damage state of the structure. The following work is an attempt at the development of a few possible objective functions to evaluate the sensitivity of a particular sensor and actuator design. This is developed from a state space framework where the damage is included as a parameter in the state space model.

### 3.2.1.1 Known likely damage areas

For areas of a structure where damage is likely to occur (also known as hotspots), the location of those areas can be exploited to generate more sensitive designs. For simplicity in the derivation, the excitation of the structure is chosen to be a zero-mean, Gaussian band-limited white noise with an input covariance matrix  $Q_u$ . This introduces energy into all of the modes of the system. The steady-state response of the system defined in 3.1 to this input is given by

$$Q_y = CQ_xC^T + DQ_uD^T \quad (3.12)$$

where  $Q_x$  is the steady-state covariance of the state vector  $x$  and can be shown to be the solution to the following matrix Lyapunov equation:

$$AQ_x + Q_xA^T + BQ_uB^T = 0 \quad (3.13)$$

Readily-available numerical algorithms exist to solve Equation 3.13. To optimally position the sensors, it was decided to maximize the matrix 2-norm of the sensitivity of the steady-state sensor covariance  $Q_y$  with respect to parametric variations in the system matrices  $A$ ,  $B$ ,  $C$ , and  $D$ . To put this plainly, the algorithm tries to maximize the change in the output signal when damage develops in the structure. Recall that, in general, the entries of these matrices are determined by the geometry and physical properties of the materials used in the structure to be monitored. The equation for this is given by

$$\frac{\partial Q_y}{\partial p} = \frac{\partial C}{\partial p} Q_x C^T + C \frac{\partial Q_x}{\partial p} C^T + C Q_x \frac{\partial C^T}{\partial p} + \frac{\partial D}{\partial p} Q_u D^T + D \frac{\partial Q_u}{\partial p} D^T + D Q_u \frac{\partial D^T}{\partial p} = 0 \quad (3.14)$$

where  $\frac{\partial Q_x}{\partial p}$  is the solution to

$$\frac{\partial A}{\partial p} Q_x + A \frac{\partial Q_x}{\partial p} + \frac{\partial Q_x}{\partial p} A^T + Q_x \frac{\partial A^T}{\partial p} + \frac{\partial B}{\partial p} Q_u B^T + B \frac{\partial Q_u}{\partial p} B^T + B Q_u \frac{\partial B^T}{\partial p} = 0 \quad (3.15)$$

and  $p$  is a parameter characterizing the effect of damage on the structure. Usually,  $p$  influences the entries of  $M$ ,  $K$ , and  $G$ . Note that Equation 3.15 is of the same form as 3.13 in its unknown and can be solved by repeated solution of a Lyapunov equation.

For this work, it was decided to model damage as a localized change in stiffness or mass of a finite element. This approach has been used by other researchers in structural health monitoring, especially in civil structure applications, and while it is not a precise means of representing a crack, it has proven to be of practical value. These parameters (stiffness and mass in a particular region of the spar) correspond to the variable  $p$  in the theoretical development described in the previous section. Ultimately, it is the goal of the design algorithm to place sensors that will maximize a measure of the output signal change given a change in these parameters.

The primary optimization criterion for known areas of likely damage,  $\left\| \frac{\partial Q_y}{\partial p} \right\|_2$ , is a measure of the change in the output power covariance in response to a structural parameter change (mass or stiffness reduction). This quantity cannot be measured



in practice; however, for small changes in  $p$ , which is what we are after, it is clear that

$$\left\| \frac{\partial Q_y}{\partial p} \right\|_2 \propto \|Q_y^{ref} - Q_y^{dam}\|_2 \quad (3.16)$$

where  $Q_y^{ref}$  and  $Q_y^{dam}$  are the reference and damaged values of the output power covariance; quantities that can be measured.

### 3.2.1.2 Global Sensitivity

If the goal of a design is to monitor all areas of a structure equally, one could just calculate a local sensitivity, as in Equation 3.16, for every element in the model and optimize over all damage cases. Since realistic models can contain hundreds of thousands of elements, this approach is computationally prohibitive. An alternate approach is to try to find the condition that produces the least-sensitive design and then maximize that case. This approach ensures that the worst-case scenario is as good as can be and also that all other cases should perform better. To develop this concept mathematically, assume a minimal state-space realization of a stable structure with any low-pass filtering effect included, then the controllability grammian  $Q$  can be obtained by solving the Lyapunov equation

$$AQ + QA^T + BB^T = 0 \quad (3.17)$$

Assuming a change in  $A$ , denoted by  $T$ , there will be a change in  $Q$ , denoted by  $S$ . Therefore, the first order variation can be written as,

$$AS + SA^T + TQ + QT^T = 0 \quad (3.18)$$

In this equation,  $S$  is the unknown quantity and it is desired to choose  $B$  in Equation 3.17 so that, for a worst-case choice of  $T$  (of fixed norm, say 1),  $S$  will be bounded away from having a zero norm, thus ensuring that there will be a change in the system's state power that can be observed by a judiciously-designed sensor network.

Choosing  $B$  to maximize the minimum singular value of  $Q$  is a sufficient choice to ensure that the norm of  $S$  will be bounded away from zero, thereby establishing that a sensor network can be chosen such that, no matter what change occurs in the system ( $A$ ), a change in the measured power will be observed.

To prove this, let  $B^*$  be the optimizing  $B$ . Then, the corresponding  $Q^*$  will be symmetric and full rank with singular value decomposition  $U\Sigma U^T$ , where  $\Sigma_{nn} = \sigma_n$  is the smallest singular value. If we let  $T = yu_n^T$ , where  $u_n$  and  $y$  are norm 1 and  $u_n$  is the singular vector corresponding to  $\sigma_n$ , then it can be shown that  $T$  is norm 1 and that

$$AS + SA^T = -\sigma_n (yu_n^T + u_n y^T) \quad (3.19)$$

Moreover, it can also be shown that  $2 \geq \|yu_n^T + u_n y^T\| \geq 1$  for all possible  $y$ . By choosing  $y$  such that  $y^T u = 0$  (orthogonality condition), the lower bound of 1 is achieved. Therefore,

$$\|AS + SA^T\| \geq \sigma_n \quad (3.20)$$

This simply states that, for all possible choices of  $T$  of norm 1, the smallest possible norm of the right-hand side is lower bounded by the minimum singular value of  $Q^*$ .

Applying the triangle inequality yields

$$\|AS\| + \|SA^T\| \geq \|AS + SA^T\| \geq \sigma_n \quad (3.21)$$

But,  $\|AS\| = \|SA^T\|$  by symmetry of  $S$ . This implies

$$2\|AS\| \geq \sigma_n \quad (3.22)$$

Applying the Schwartz inequality yields

$$2\|A\| \|S\| \geq 2\|AS\| \geq \sigma_n \quad (3.23)$$

Finally, we get

$$\|S\| \geq \frac{\sigma_n}{2\|A\|} \quad (3.24)$$

Thus, we see that the norm of  $S$  is lower bounded by the smallest singular value of  $Q$ . Therefore, it is desirable to maximize its value to ensure sensitivity to unknown changes  $T$  in the system matrix  $A$ . In other words, it is necessary to maximize the minimum singular value of that sub-matrix of  $Q$  that corresponds to the states that

are potentially measurable by a sensor network. Doing so requires the extraction of the appropriate rows and columns of  $Q$  in order to form the smaller matrix, say  $Q_m$ .

### 3.2.2 Minimum Number of Sensors

The objective function to minimize the number of sensors is simply the number of sensors used in the design. Other factors like size, weight, and cost can also be included here, which is especially useful when trying to determine between different sensors of the same type (i.e., two different brands of strain gauges). This is so trivial as to almost be omitted; however, for completeness it is included here.

### 3.2.3 Robustness

When optimizing with respect to models-especially models that may have gross errors, it is desired for the design's performance to be robust to modelling error. Another way to say this is that the designs should be minimally sensitive to the parameters that define the model. At first, this may seem contradictory to the sensitivity objective case, but another way to think of it is that it is desired to have the designs sensitive to *changes* in the parameters of the model while not necessarily the particular values of those parameters. This being said, the robustness objective is typically a trade-off with sensitivity. To formalize this mathematically, the sensitivity function of Equation 3.15 is implicitly differentiated with respect to a global parameter  $g$ . This leads to the following equation

$$\begin{aligned}
& \frac{\partial^2 A}{\partial p \partial g} Q_x + \frac{\partial A}{\partial p} \frac{\partial Q_x}{\partial g} + \frac{\partial A}{\partial g} \frac{\partial Q_x}{\partial p} + A \frac{\partial^2 Q_x}{\partial p \partial g} + \frac{\partial^2 Q_x}{\partial p \partial g} A^T + \frac{\partial Q_x}{\partial p} \frac{\partial A^T}{\partial g} + \frac{\partial Q_x}{\partial g} \frac{\partial A^T}{\partial p} + Q_x \frac{\partial^2 A^T}{\partial p \partial g} \dots \\
& + \frac{\partial^2 B}{\partial p \partial g} Q_u B^T + \frac{\partial B}{\partial p} \frac{\partial Q_u}{\partial g} B^T + \frac{\partial B}{\partial p} Q_u \frac{\partial B^T}{\partial g} + \frac{\partial B}{\partial g} \frac{\partial Q_u}{\partial p} B^T + B \frac{\partial^2 Q_u}{\partial p \partial g} B^T \dots \\
& + B \frac{\partial Q_u}{\partial p} \frac{\partial B^T}{\partial g} + \frac{\partial B}{\partial g} Q_u \frac{\partial B^T}{\partial p} + B \frac{\partial Q_u}{\partial g} \frac{\partial B^T}{\partial p} + B Q_u \frac{\partial^2 B^T}{\partial p \partial g} = 0
\end{aligned} \tag{3.25}$$

This gives the sensitivity of the design to the global parameters that were used in the model. In cases where the initial model may be wildly inaccurate, it may be useful to also look at the second derivative to see if the curvature is high; if it is, then an alternative design should probably be selected.

### 3.3 Genetic Algorithm

Genetic algorithms (GA) attempt to find solutions to problems by mimicking biological evolutionary processes, with a cycle of random mutations yielding successive generations of “solutions.” While there are several approaches to estimating solutions to MOO problems, approaches based on evolutionary programming and genetic algorithms have become the most popular, [9, 13, 15, 18, 34, 41], due to their flexibility and ease of implementation. Genetic algorithms are a stochastic global search method that mimics natural selection. GAs operate on a population of potential solutions applying the principle of survival of the fittest to produce increasingly improved approximations to a solution. At each generation, a new set of approximations is created by selecting individuals according to their level of fitness in the problem domain and “breeding” them together. This is done by taking a large selection of random points that cover all the ranges of all the input parameters and

evaluating each of them. Then, the best points are selected and a new generation of points is created by some heuristic from the first set, and the next generation is evaluated. Since the new points are chosen from the best of the previous generation, these algorithms improve with each successive generation of points. The algorithms generally run for a fixed number of generations, and the best points will generally be close to the Pareto Surface.

Individuals in the population are called chromosomes and they are encoded in a way that makes sense to a particular problem. Assessing the fitness of a particular chromosome is done through objective functions that characterizes an individual's performance in the problem domain. This value is used in the selection to help choose more fit individuals. Highly-fit individuals have a high probability of being selected for mating, whereas less fit individuals have a low probability of being selected for mating. Once individuals are selected for mating, genetic operators manipulate the genes of the chromosome, using the assumption that certain individual's gene codes, on average, produce fitter individuals; this is called recombination. Another operator is genetic mutation. Mutation causes the individual genetic representation to be changed according to some probabilistic rule; this has the effect of tending to limit the possibility of converging to a local optimum.

For this study, it was chosen to encode the GA's chromosome such that every gene was an integer location on a finite element model. The number of genes in a chromosome depended on the maximum number of sensors to be considered. Since we were interested in finding a Pareto surface that would compare different design trade-offs,

including how many sensors to use, a zero in any gene meant that one less sensor was used. The objective functions used to evaluate the fitness of a chromosome were the four metrics derived previously in Section 3.2. They included the local and global sensitivities, design robustness, and the number of sensors used. A population of 200 individuals was used with the initial chromosomes being assigned by a uniform distribution. Stochastic universal sampling (SUS) was used to select which chromosomes to breed. SUS is a single-phase sampling algorithm with minimum spread and zero bias. The offspring were created using discrete recombination and the mutation rate was set at 6%. Once the offspring were created, they were fully reintroduced with their parent population and a search for the top non-dominated designs were done. Once these Pareto designs were found, they were assigned to sub-populations along with their closest neighboring designs so that the Pareto surface could be evolved more efficiently. Along with the mutation rate there was a migration rate of 0.02% between the sub-populations to ensure that global minima were found.

### **3.3.1 Finding the Pareto Surface in the Context of a Genetic Algorithm**

A typical genetic algorithm requires the definition of a genetic representation of the solution domain (i.e., definition of the chromosome structure) and a fitness function to evaluate the solution domain. When determining a solution to satisfy a single objective, this fitness function can simply serve to indicate the individuals in a genetic algorithm's population that are associated with the maximum or minimum objective values. This imposes a pressure on the population of the genetic algorithm,

forcing its otherwise random evolution into a direction that gives rise to solutions that represent local or global maximums or minimums, depending on the intended direction of the optimization.

In the case of multiple objectives, the fitness function needs to be defined such that it gives precedence to non-dominated solutions over dominated solutions [27]. These non-dominated solutions, by definition, represent the Pareto optimal surface given in Equation 3.11. However, simply defining the solutions on the Pareto surface as having a better fitness value than dominated solutions does not create the genetic pressure necessary to ensure that the genetic algorithm converges to solutions that are representative of the overall Pareto optimal surface.

Instead of spreading out across the entire Pareto surface, the solution set present in the population of the genetic algorithm tends to cluster around a region of the Pareto surface. In order to prevent this, an additional genetic pressure is necessary in order to increase the entropy of the solution set. This is achieved by the following Pareto genetic algorithm pseudo-code:

- Choose an initial population;
- Find non-dominated individuals in population;
- Eliminate duplicate non-dominated individuals and replace them with new randomly generated individuals;
- Assign a fitness value of 1 to all non-dominated individuals, 0 to all others; and
- Repeat:
  - Select best-ranking individuals to reproduce
  - Breed new generation through crossover and mutation and give birth to offspring
  - Replace dominated individuals with offspring



- Find non-dominated individuals in population
  - Eliminate duplicate non-dominated individuals and replace them with new individuals
  - Assign a fitness value of 1 to all non-dominated individuals, 0 to all others
  - Check objective distances between all individuals
  - Select the  $N$  non-dominated individuals that are the “most” equidistant from each other while preserving the endpoints
  - Set the fitness value of the remaining non-dominated individuals to 0;
- Until some terminating condition.

Here,  $N$  is some parameter set by the user indicating the number of points desired to represent the Pareto surface. Looking at this pseudo-code, a few things become apparent. First, duplicate non-dominated individuals are eliminated from the population each iteration; this prevents the advent of an elitist or homogeneous population. Second, only the  $N$  non-dominated individuals that are the farthest objective distance apart are given a non-zero fitness value. Both of these impose a genetic pressure on the population that encourages the solution set in the population to effectively “spread out” across the Pareto surface, thus ensuring that points don’t “clump” together in one area of the solution space. Since the purpose of optimization is to find some unknown “best” solution, it is sometimes difficult to know when that solution is found. As such, some consideration should be given to the terminating condition. There is typically “no one size fits all” criteria but some rules-of-thumb that depend on the size and topology of the solution space. One way to decide to terminate is to watch the evolution of solutions to see if they reach a steady-state. This does not guarantee that the optimal solution is reached as it could be a local minima. Alternatively, one could also run the algorithm multiple times to see if it

converges to the same set of solutions. Another way is to just assign a fixed number of generations and take the best set of solutions at that point. The number of generations assigned this way is typically based on human experience and judgment. This last method was employed in this work as experience showed that between two hundred and five hundred generations was sufficient for small sized problems.

## CHAPTER 4

### RESULTS

This chapter ties together all the disparate parts in the methodology to create an optimal set of sensor and actuator designs for the purpose of monitoring the health of structural components. Different analysis will be done via simulation to explore the effectiveness of the different objective function formulations. The optimality of the design produced will be compared to an exhaustive search using a simplified model. A more realistic case with many possible local minima will also be evaluated by first fixing some of the free design parameters and then doing an exhaustive search over the remaining ones. The robustness objective function will be evaluated using Monte Carlo simulation where different models are created. Note that the models used in the evaluation process are perturbed versions of the one used for the design.

The objective functions for local and global sensitivity, minimum number of sensors, and robustness will be used to find the Pareto set of designs that represent the optimal trade-offs in the design space. The optimization is performed using a genetic algorithm set up as laid out in Section 3.3. This will be done for three different components that are replicas of common structures found in aerospace applications. Once the Pareto set of design is found for each structure, one particular design is chosen for implementation. In each case, the chosen design will be simulated to eval-

uate its performance with respect to the design objectives and then an experiment will be carried out.

The experiments will consist of taking enough data in an undamaged reference state to establish the baseline statistics. Once these statistics are known, damage will be introduced and a statistical hypothesis test will be done to determine if the system successfully detects the damage. The introduced damage will typically be in the form of a cut (which simulates a crack), a change in mass (which approximates corrosion), or a bolt loosening. A comparison will also be performed between an optimally design system and one designed by a human using some heuristics.

#### **4.1 Model**

For all practical purposes, any modeling method that can be finessed into the standard linear state space form can use this design method. This includes linear elastic finite-element (FE) methods, finite-difference (FD) heat transfer modeling, and finite-difference time-domain (FDTD) methods. While this is true in general, this work will use specific models to highlight the concepts of Chapter 3. For this work, three different models will be used: a helicopter roof strap that holds two bulkheads together; a helicopter landing gear; and a wing attachment fitting that typically connects an airplane wing to the fuselage.

Each finite element model is a linear elastic structural model. The roof strap test article was designed to be a close replica of an actual roof strap and the boundary conditions as they are on the vehicle. This involved creating detailed drawings of

the roof strap, as well as bulkheads, stiffeners, and supports. The roof strap and its test stand (modeled for accurate boundary conditions) were meshed with shell elements. Beam elements were used to join the roof strap and test stand at fastener locations. Both element types have six degrees of freedom (three translational and three rotational) at each node. A plane of symmetry allowed for modeling one-half of the roof strap test set-up. The landing gear is primarily a hollow cylindrical structure and was also meshed with shell elements. Point mass elements were used on both ends of the landing gear model to approximate the mass of a rectangular base and an attachment fitting at the opposite end. The wing attachment fitting was meshed with hexahedral and tetrahedral solid elements having only translational degrees of freedom. Hexahedral elements were used in regularly shaped regions to minimize the model degrees of freedom and tetrahedral elements used in complexly shaped regions. The number of degrees of freedom for the roof strap, landing gear, and attachment fitting finite element models were 37099, 13746, and 33178, respectively.

Once the drawings for the articles were complete, Finite-Element Modeling (FEM) was initiated using ANSYS™. ANSYS™ is a commercially-available general purpose finite element modeling package for solving a wide variety of mechanical problems. Types of problems solved by ANSYS™ include static/dynamic structural analysis (both linear and non-linear), heat transfer and fluid problems, as well as acoustic and electromagnetic problems. All models generated for this program were linear elastic-based models. Since a free-free state was chosen for the testing of the landing

gear, no additional boundary conditions were added to the model. The roof strap, however, has many boundary conditions resulting in a very stiff structure.

#### 4.1.1 Model Refinement

Given that the design methods here are, to an extent, model-dependent, care should be taken in developing good models. Model refinement is an important step in avoiding the garbage in, garbage out phenomena. After each model was developed, various modal analysis tests were performed. Impact hammer, sine sweep, and sine chirp inputs were used to establish the modes of each test article. These modes were then fed back to the modeler in order for the models to accurately represent the dynamics of the test articles. The impact hammer test was performed by impacting each test article in various locations and recording the dynamic response using accelerometers placed along the length of article. Sine sweep and sine chirp tests were performed by inputting a sine sweep or chirp function into the test article via a piezo-electric disc. The response to this input was captured the same manner and at the same locations as the impact hammer test. These results were analyzed and compared to the results of each FE model. By exporting the mass and stiffness matrix from ANSYS™, an eigen-decomposition was performed to extract the natural frequencies and mode shapes of each model. The accuracy was then determined by comparing the displacement at each accelerometer's physical location in the model to what was actually measured during the dynamic tests. The model was then refined to reduce the error between the displacements as much as possible.

## 4.2 Design Surface

After the models were updated to represent the dynamics of the test articles as closely as possible, an optimized structural health monitoring design was developed.

In doing so, the following information was determined:

- the frequency band for which the model is valid;
- the potentially measurable degrees of freedom via accelerometers; and
- the degrees of freedom that were potentially usable for force actuation.

To design an optimal system for detecting damage, metrics for quantitatively assessing the quality of a design were defined. To be effective, these metrics were closely associated with physically meaningful quantities. For detection, the metric must be a quantity that can be physically measured. Our metrics focused on the information provided in the power covariance matrices. Because models are always, to some degree, approximations, the approach taken was that detection should be based on changes in measurable quantities from baseline statistics rather than absolute values. Such methods are far more tolerant to modeling error. All such change-based methods are based on sensitivity-type calculations. In particular, the area of interest was the sensitivity of the output measurements to changes in the system. In this case, the changes were represented by the mass and stiffness matrices, which are in turn defined in terms of material properties and geometry. In general, the key sensitivity with respect to any metric is the partial derivative of the output with respect to the parameter of interest. In the case of the landing gear, the location and nature of the anticipated damage was not defined. Since the part needed to

remain in its original undamaged state, it was decided that damage would be introduced only by placing magnets on the part in any location. An optimal input/sensor combination was developed that would achieve adequate damage detectability over the entire structure. To do this, the system was designed to have good controllability and observability in the traditional sense, i.e., the grammians for the system had the appropriate structure. In essence, what was required was that the minimum Hankel singular values of the system (the Hankel singular values are the square roots of the singular values of the product of grammians) were bounded away from zero. All of these design issues were addressed through appropriate application of design optimization algorithms for proper sensor/actuator locations. For the roof strap, the damage location was known. This allowed another step to be added in addition to optimizing the observability and controllability grammians. Cracking causes a reduction in stiffness in the area where it is occurring; therefore, the partial derivatives, with respect to stiffness in the elements where damage was to be created, were found. By optimizing the observability and controllability grammians as well as the sensitivity to known damage location, it was possible to design a structural health monitoring system for the roof strap that was maximally sensitive to anticipated and unanticipated damage.

#### **4.2.1 Design Results**

The multi-objective genetic algorithm was used to design health monitoring systems for two components. The first component is a representative landing gear, as



illustrated in Figure 4.1. The objectives of the design were to place sensors and actuators to detect damage anywhere on the structure and to maximize the design's robustness to modeling error. The design algorithm was limited to placing two one-axis accelerometers and one piezo-electric transducer to meet all the objectives. Also shown in Figure 4.1 are the sensor and actuator locations, as determined by the design algorithm and a human designer. The two optimal sensors and actuator, as determined by the genetic algorithm, are shown in red and yellow respectively. A human was asked to design a system (shown in purple) to meet the same objectives and was allowed four accelerometers to design with but was limited in that the actuator location was fixed to the location chosen by the genetic algorithm.

The second component for which a design was implemented was a roof-strap surrogate for a helicopter, as shown in Figure 4.2. A roof-strap is a structural component that holds two bulkheads together and can experience a lot of fatigue during certain maneuvers. This time, the design objectives were to maximize sensitivity to expected damage, as shown in orange in Figure 4.2, and to detect damage anywhere else in the structure while producing designs that were robust to modelling error. Again, the algorithm was limited to placing two one-axis accelerometers and one piezo-electric transducer to meet all the objectives. Figure 4.2 shows the sensor and actuator locations as determined by the design algorithm and the human designer. The two optimal sensors and actuator as determined by the genetic algorithm are shown in red and yellow, respectively. Again, the human was allowed four accelerom-

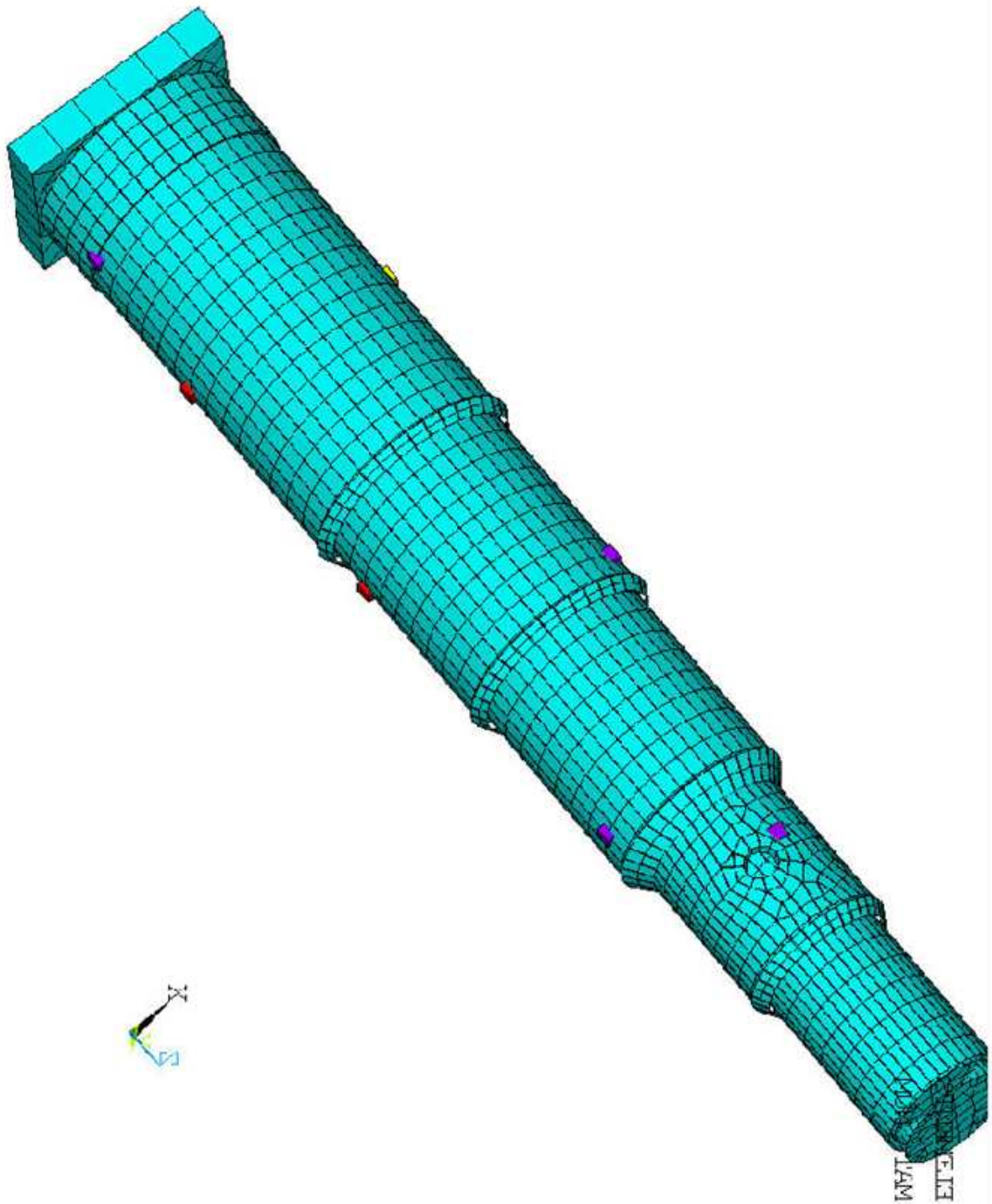


Figure 4.1  
Landing Gear Designs

eters but was limited in that the actuator location was fixed to the location chosen by the GA. The locations of the sensors in this design are shown in purple.

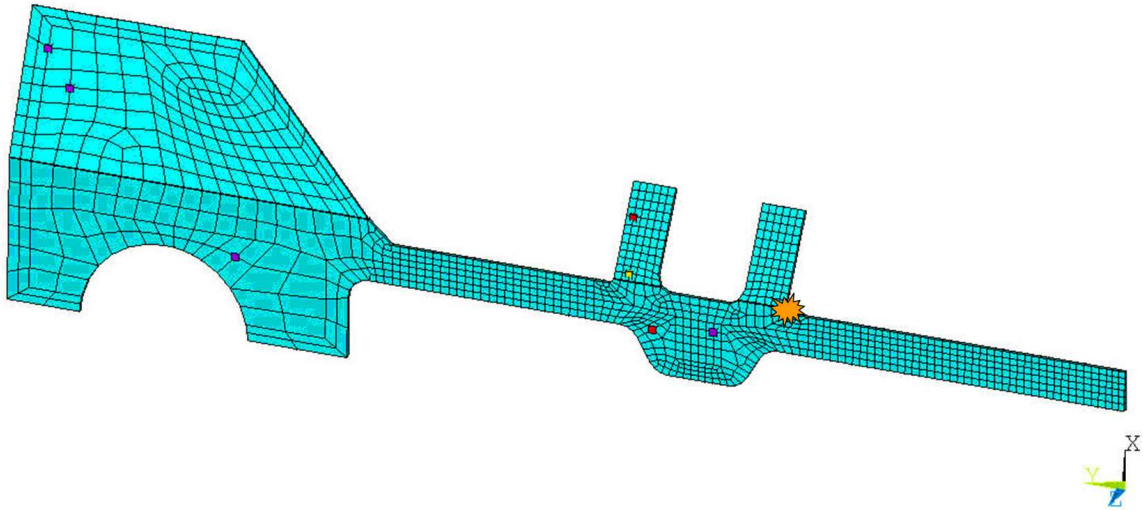


Figure 4.2

### Roof Strap Designs

A third design was made for a wing attachment fitting surrogate. On a typical aircraft, the fitting connects the outer wings to the center wing. The designs were optimized to detect damage at a known crack initiation point on the center board cut-out as highlighted in green on Figure 4.3. Other objectives included: number of sensors, robustness to modeling error, and observability of unexpected damage. A design, which is shown in Figure 4.3, was chosen based on its balance of all objective and simulated performance from the Pareto set that used four accelerometers (shown in purple) and one piezo-electric actuator (shown in red). Thermocouples, shown in

orange, were included in this experiment to monitor for hidden variables such as the environmental temperature.

#### 4.2.2 Evaluating Design Optimality via Exhaustive Search

To evaluate this placement algorithm, the results from a design optimization are compared to an exhaustive search of all possible solutions. This is often not possible due to the size of typical models; however, for purposes of examination, a simple model of a cantilever beam was created. The model is of a sufficiently small size to ensure that an exhaustive search is feasible. An illustration of the beam is provided in Figure 4.4.

The beam was modeled using the properties of 1080 steel with dimensions  $457.2 \text{ mm} \times 50.8 \text{ mm} \times 6.35 \text{ mm}$ . A 36-element (72 DOF) finite-element model of the undamaged beam was developed using Euler-Bernoulli beam elements. The parameters of the design were to place one sensor to best detect damage modeled as a reduction in the stiffness at element 32 given that a single input random excitation was assumed to be at node 36. The required partial derivatives were calculated and the optimal placement (maximizing the 2-norm of Equation 3.16) was performed using a genetic algorithm. The single-sensor sensitivity was then calculated for every location along the beam and compared against the genetic algorithm's solution. In this case, the GA determined the global optimal solution. It should be cautioned that this will not necessarily be the case in every problem because GAs, unlike some other optimization schemes, have no guarantee of finding the global minimum.

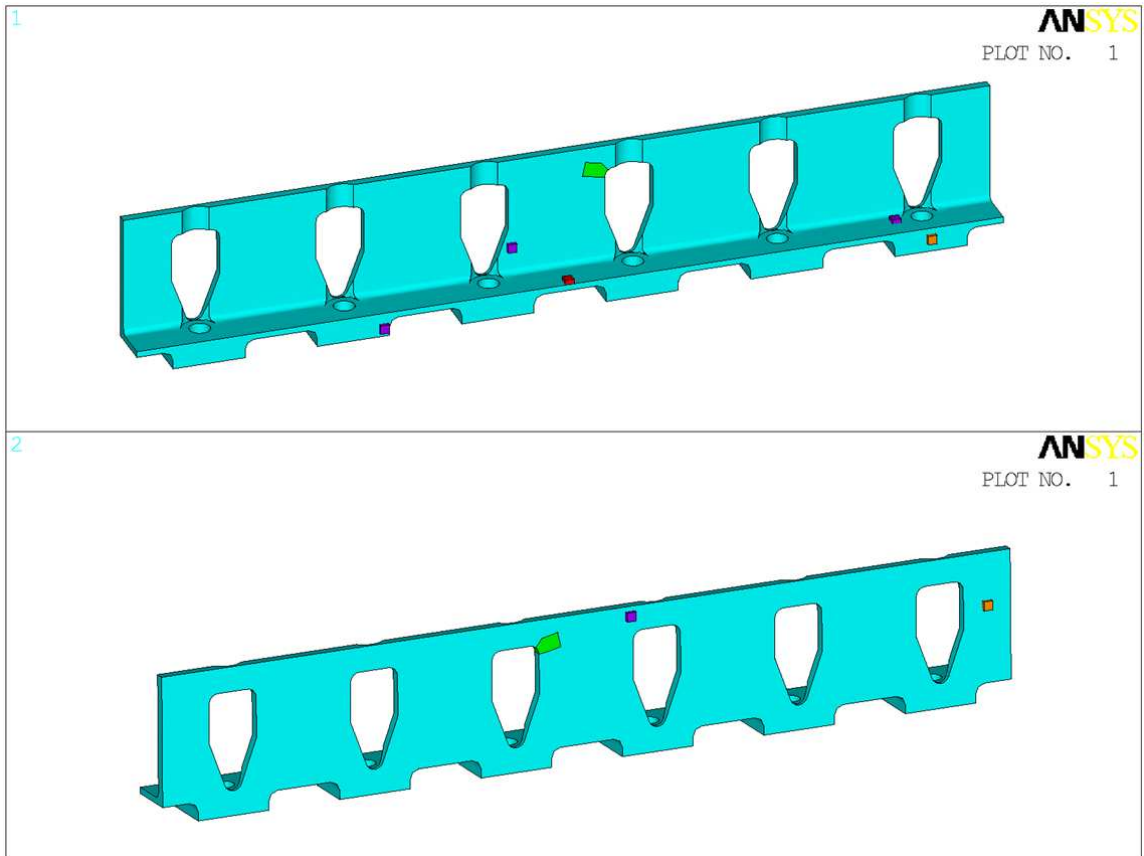


Figure 4.3

Surrogate Rainbow Fitting Design

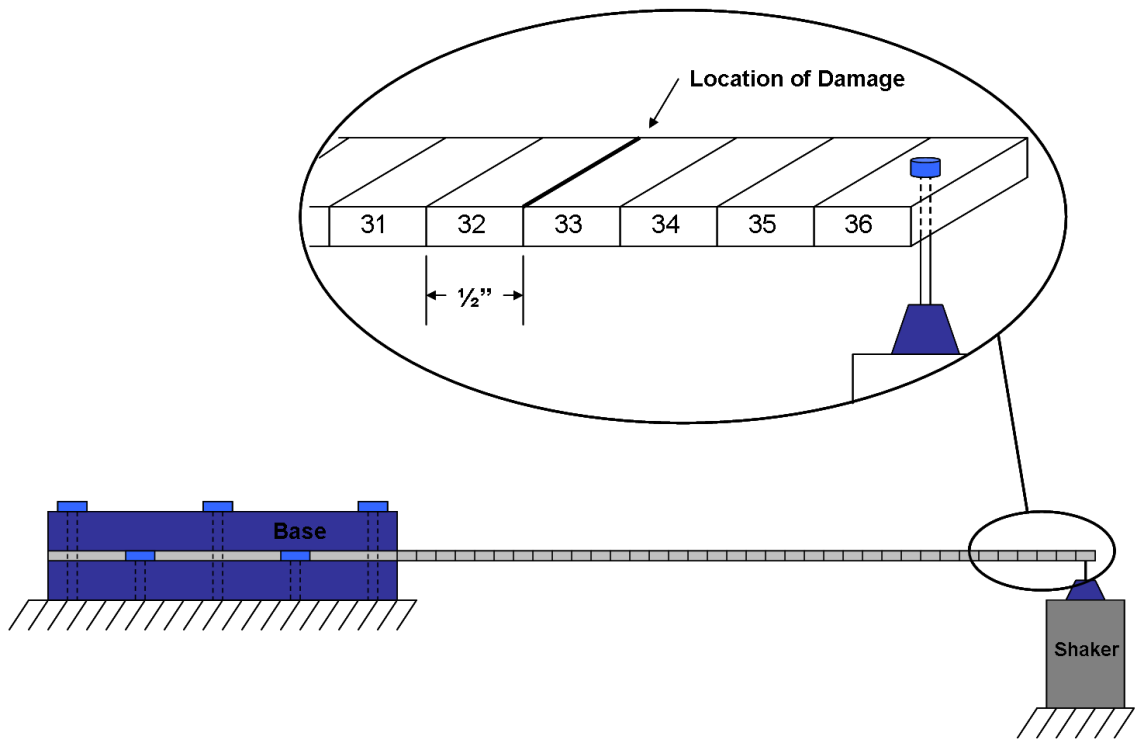


Figure 4.4

Simple Cantilever Beam Model

In order to determine how well the optimization algorithm would perform on a typical problem with many local minima, a design was done for the wing attachment fitting. Design parameters were made as follows: to use between two to six sensors, maintain observability to damage anywhere, be robust to modeling errors, and be maximally sensitive to damage occurring in an inboard cut-out. The final design is shown in Figure 4.3 with the expected damage area highlighted in green. Because of the large number of possible solutions in the design space, approximately  $4^n/(n-6)!$  where  $n = 33178$ , an exhaustive search would be out of the question. Instead, the finite element model of the surrogate was used to perform an exhaustive search of the sensitivities of the health monitoring system for the fixed four-sensor design and only along the surface of the part. This required computing the sensitivity,  $dQ_y$ , for every finite element, where  $dQ_y$  is a measure of the health monitoring system's ability to detect a change in the elastic modulus of a finite element. Figure 4.5 is a contour plot of  $dQ_y$  and tells us that the model's sensitivity to damage is highest at the center of the surrogate, precisely where it was designed to be, and decreases towards each end. While this isn't exactly the same as an exhaustive search of the total design space, it is the equivalent of doing so over one objective function and it does demonstrate that the optimization did maximize the sensitivity objective, as it was designed to do.

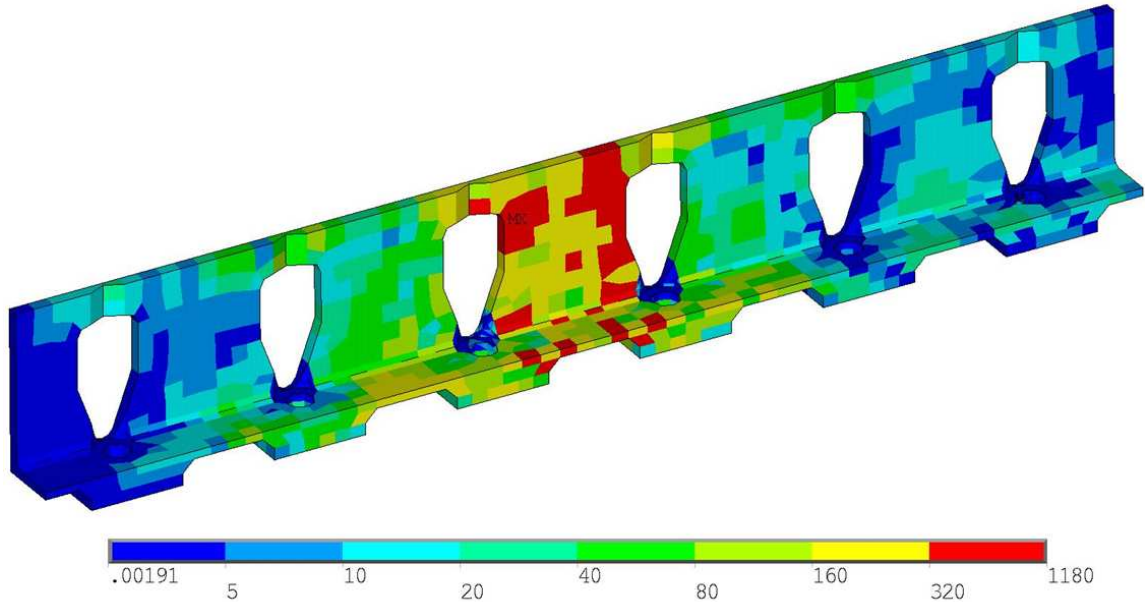


Figure 4.5

Contour Plot of  $dQ_y$

### 4.2.3 Evaluating Design Robustness

One quality of a well-designed structural health monitoring system is that the implementation is robust enough such that inaccuracies in the initial assumptions (i.e., modeling parameters or boundary conditions) minimally affect the other performance objectives of the health monitoring system. It is understood that all changes will affect the performance to some degree and that if a design is truly optimal, the performance should decrease (as opposed to a performance increase); however, the performance decreased should be minimized to the extent possible. This minimization method was laid out in Section 3.2.3 and can be used during the design stage by only implementing the optimal designs from the Pareto set with the lowest sensi-



tivity to these errors or by including an objective function in the optimization that explicitly tries to minimize it. This section will attempt to evaluate the effectiveness of the robustness criteria laid out in 3.2.3. A few possible evaluation methods are as follows:

1. Numerically calculate the sensitivity;
2. Calculate the analytical sensitivity; or
3. Perform a Monte Carlo analysis to analyze the sensitivity.

These methods range from the conceptually simple to an in-depth analysis using statistical methods. This effort shall focus on methods 1 and 3 because method 2 is quite often impossible due to the fact that, unless a model is trivial, there are rarely closed-form solutions with which to analytically derive the sensitivity.

#### **4.2.3.1 Evaluating the Design Sensitivity Numerically**

To numerically estimate the sensitivity of a design to the design assumptions, Newton's difference quotient was applied. This states that the derivative is the value of the difference quotient as the secant lines approach the tangent line. This can be mathematically expressed as

$$f'(a) = \lim_{h \rightarrow 0} \frac{f(a+h) - f(a)}{h} \quad (4.1)$$

where  $f(a)$  is the system performance at the reference design parameters  $a$  and  $h$  is a perturbation in the design parameters. As long as  $h$  is sufficiently small,  $f'(a)$  will be a good approximation of the sensitivity of the designs to changes in the

initial assumptions. Once the sensitivity is known it can be multiplied by what a typical error in the initial assumptions to analyze the effect in terms of worst-case performance loss. Calculating the sensitivity for the 5-sensor design used on the wing fitting surrogate with respect to density yields the symmetric matrix sensitivity of

$$\begin{array}{ccccc}
 -405 & -1290 & -889 & -3637 & -592 \\
 & 420 & -1120 & -1807 & -1291 \\
 & & 931 & 865 & 350 \\
 & & & -5690 & 1777 \\
 & & & & -505
 \end{array} \tag{4.2}$$

with a matrix 2-norm of 8.2E3. This roughly means that, if the material density used for the initial design was off by one pound per cubic inch, then the sensitivity of the damage metric to cracking at one of the hotspots would be reduced by 8.2E3. This may initially seem like a lot until it is realized that being off by one pound per cubic inch is an astronomical amount. In typical cases, even if the material properties varied as much as 20% (which is significantly higher than current manufacturing process tolerances) from the reported densities, it would only result in a change in about 5.3E-5 pounds per cubic inch. Therefore, in the case of the fitting, if the density used in the model was off by 20%, the sensitivity would be reduced by roughly 0.4. Given that experimentally the damage metric was  $\sim 3E4$  after a very small amount of damage, a reduction in sensitivity by 0.4 amounts to a 1.3E-3% loss in sensitivity. For a very large amount of damage, the damage metric was  $\sim 12E4$  so the loss in

sensitivity would have been  $\sim 3.3\text{E-}4\%$ . For comparison, the electronic and process noise for the equipment used in the experiment was  $6.4\text{E}3$ . This means that the sensitivity loss is less than the noise of the measurements, showing that the derived objective function for determining robustness has merit.

Carrying out a similar set of calculation for loss of sensitivity due to incorrect assumptions about the material's modulus yields a symmetric matrix sensitivity of

$$\begin{array}{ccccc}
 -3.4 & 2.8 & 1.2 & -0.91 & -0.068 \\
 & -1.9 & 4.8 & 3.0 & 2.9 \\
 & & -2.4 & -7.8 & -0.56 \\
 & & & -1.4 & -2.7 \\
 & & & & -1.9
 \end{array} \times 10^{-8} \tag{4.3}$$

with a 2-norm of  $1.3\text{E-}7$ . Again, this roughly means that if the Young's modulus was different from the datasheet by 1 psi, then the sensitivity of the damage metric to cracking at one of the hotspots would be reduced by  $1.3\text{E-}7$ . This may seem small, but it is the opposite effect of the density in that 1 psi is very small when talking about the Young's modulus of aircraft aluminum which is typically on the order of magnitude of  $10\text{E}7$  or greater. Following the previous argument, a 20% variation from the datasheet would result in a change of  $2.0\text{E}6$  psi. In the case of the wing fitting, the published modulus being 20% off from the actual would reduce the damage metric by 0.26. Given that experimentally the damage metric was  $\sim 3\text{E}4$  for small amounts of damage, a reduction in sensitivity by 0.4 amounts to an  $8.6\text{E-}4\%$

loss in sensitivity. Comparing again to the electronic and process noise of 6.4E3, the sensitivity loss is less than the noise of the measurements, again showing that the derived objective function for determining robustness has merit.

#### **4.2.3.2 Monte Carlo Evaluations of Design Sensitivity**

A Monte Carlo analysis was done to independently assess the effectiveness of the robustness criterion laid out in Section 3.2.3. Monte Carlo methods are a class of computational algorithms that rely on repeated random sampling to compute their results. Monte Carlo methods are often used when simulating physical and mathematical systems. Monte Carlo methods tend to be used when it is unfeasible or impossible to compute an exact result with a deterministic algorithm. More broadly, they are useful for modeling phenomena with significant uncertainty in inputs, which is the type of case we are studying. There is no single Monte Carlo method; instead, the term describes a large and widely-used class of approaches. However, these approaches tend to follow a particular pattern, which is generally as follows:

1. Define a domain of possible inputs;
2. Generate inputs randomly from the domain using a certain specified probability distribution;
3. Perform a deterministic computation using the inputs; and
4. Aggregate the results of the individual computations into the final result.

In this case, the domain of possible inputs will be defined to be a 20% variation of the nominal physical parameters. For example, if the model used to generate the Damage Monitoring System (DMS) had a density of 1, then the domain of the

simulation would be densities between 0.8 and 1.2 following a Gaussian distribution (see Figure 4.6). A Gaussian distribution was chosen since it has maximum entropy for a continuous random variable. 1000 random samples were selected, generating 1000 new models of the wing fitting, and the sensitivity of the designs were computed through simulation. All the results were then collected together as a distribution of sensitivities. Entropy was used to analyze the results. In information theory, entropy is a measure of the uncertainty associated with a random variable; as such, low entropy means less uncertainty or more organization of a distribution. Therefore, in this Monte Carlo simulation, the parameters of the model have an entropy value and if the distribution of sensitivities has a lower entropy, that means that even though there was higher uncertainty in the model (high entropy), the resulting design produced approximately the same results (low entropy).

For this evaluation, the models and DMS design for the wing attachment surrogate will be used, as seen in Figure 4.3. Figure 4.6 shows the distribution of the densities used in 1,000 models of the analysis. The entropy of the densities was -2.41. Figure 4.7 shows the resulting sensitivities for the 1000 simulations run using all the models generated from the density distribution. The entropy of the resulting distribution was -8.76, which was less than the generating distribution. This shows that even though there was a lot of uncertainty in the input, the output had more structure (less uncertainty). At first, it was surprising that the output distribution was not Gaussian like the input one but Figure 4.8 demonstrates why that was not the case.

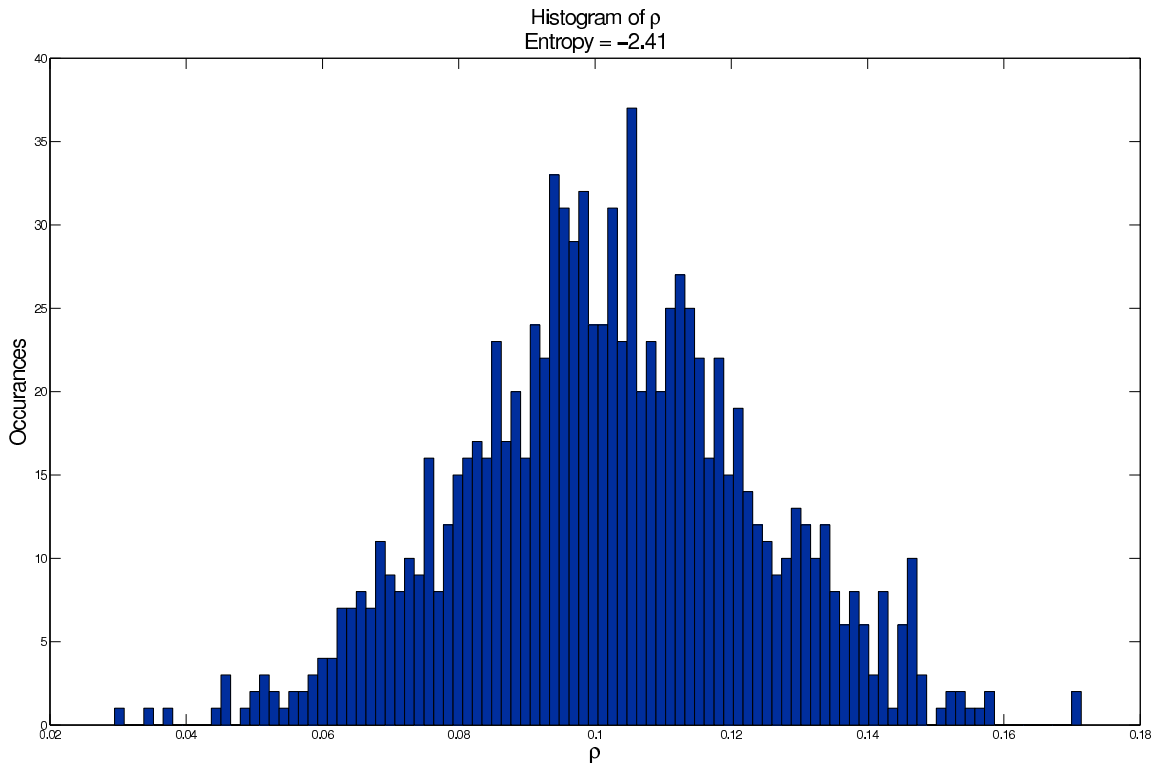


Figure 4.6

Histogram of Model Density

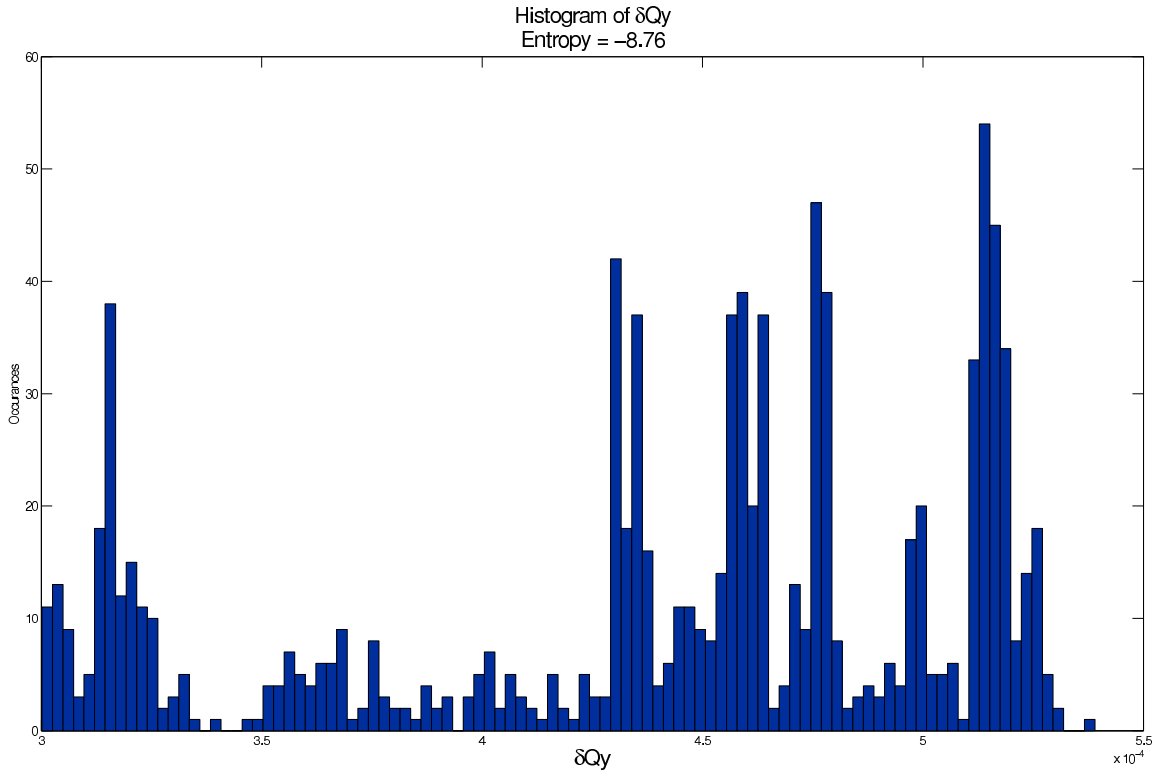


Figure 4.7

Histogram of Sensitivities

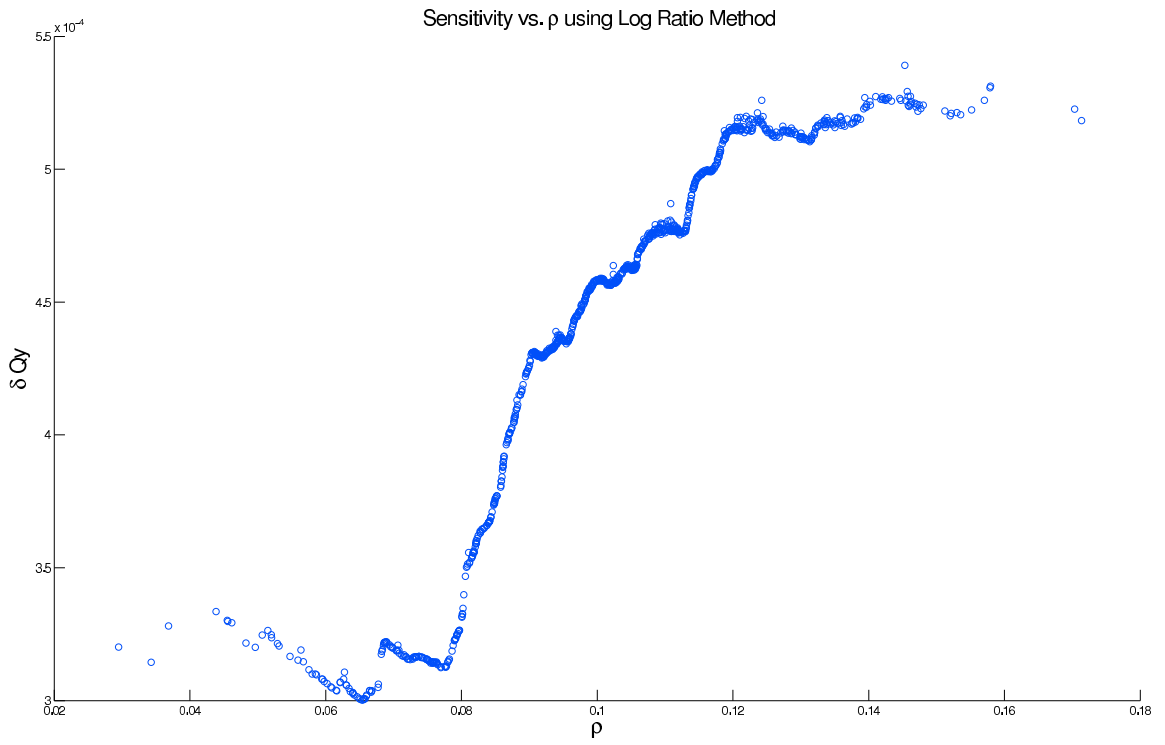


Figure 4.8

Sensitivity vs. Density



The data in Figure 4.8 was generated using the histogram of Figure 4.7. One can see that the sensitivity varies are approximately linear at around the nominal density of 0.1, but as one moves to the extremes of the histogram, the sensitivity saturates at a high and low value. Since this is a non-linear behavior, one would not expect a Gaussian distribution as the output given a Gaussian input.

The same analysis was performed for variations in the modulus of the material. After the lessons learned from the first Monte Carlo simulation, the second analysis was able to be done using much less points. Figure 4.9 shows the results. The entropy of the initial and output distributions was 15.38 and -7.96, respectively, showing again that the designed DMS produced about the same sensitivity even though the parameters of the model varied greatly from the one used in the initial design.

When compared to previously-collected data on a wing fitting, all the predicted variations due to the modeling error are below the noise inherent in the data acquisition (DAQ) system used to collect the data. This is a very favorable outcome and it shows that the effects of modeling error can be mitigated by using the robustness objective function.

The techniques highlighted here are good for evaluating the sensitivity of a design to the design assumptions (density, modulus, etc.) but are cumbersome for incorporating into the optimization algorithms due to the need to create perturbed models to evaluate the sensitivities. A simplified way to incorporate this into optimization

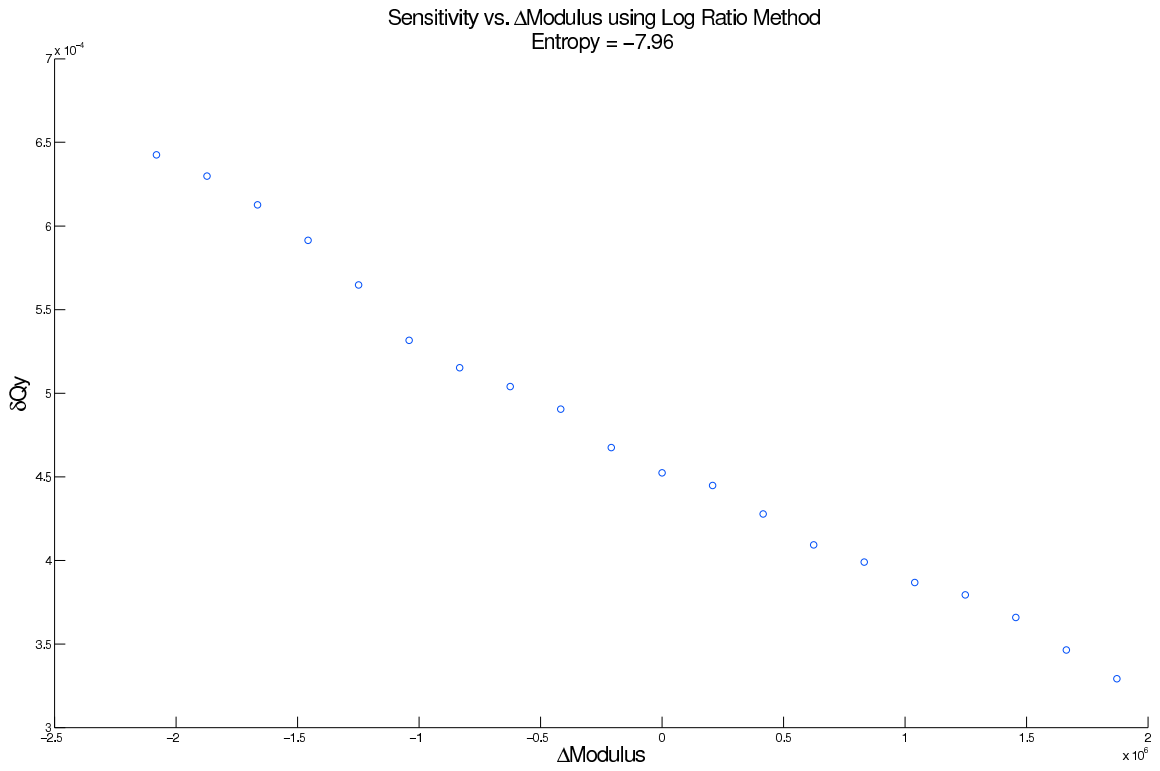


Figure 4.9

Sensitivity vs. Modulus

algorithms would be to analytically calculate the sensitivity and include that as an objective, as laid out in Section 3.2.3.

### 4.3 Simulated Results

#### 4.3.1 Simulated Damage Detection

To test how well the GA's optimal solutions performed, a simulation was done using the models and designs for the landing gear and roof strap, as seen in Figure 4.1 and Figure 4.2, respectively. Simulations for each test article were performed by generating the output covariance matrix as a baseline, and then plotting the two norm of the difference between the baseline and the next output covariance matrix, per Equation 3.16. Each optimal design consisted of one actuator and two accelerometers. The response of these optimal designs was compared to four heuristically-placed accelerometers responding to the same actuator as the optimal sensors.

The simulation was done by using Newmark's method to simulate the time response of the models given by Equation 3.2. The Newmark method is a numerical integration method used to solve differential equations. It is commonly-used by finite element programs for transient analysis. Using Newmark's method, the displacements ( $x$ ) and velocities ( $\dot{x}$ ) are approximated as

$$x_{n+1} = x_n + \dot{x}_n \Delta t + \left[ \left( \frac{1}{2} - \alpha \right) \ddot{x}_n + \alpha (\ddot{x}_{n+1}) \right] \Delta t^2 \quad (4.4)$$

$$\dot{x}_{n+1} = \dot{x}_n + [(1 - \delta) \ddot{x}_n + \delta (\ddot{x}_{n+1})] \Delta t \quad (4.5)$$

where  $\alpha$  and  $\delta$  are parameters that determine the stability of the scheme, and  $\Delta t = t_{n+1} - t_n$  is the integration time step. The parameters  $\alpha$  and  $\delta$  define a family of methods. Using values of  $\frac{1}{4}$  and  $\frac{1}{2}$  for  $\alpha$  and  $\delta$ , respectively, is known as the constant average acceleration method and is unconditionally stable. Equation 4.4 can be rewritten as

$$\ddot{x}_{n+1} = \frac{1}{\alpha\Delta t^2} (x_{n+1} - x_n) - \frac{1}{\alpha\Delta t}\dot{x}_n - \left(\frac{1}{2\alpha} - 1\right)\ddot{x}_n \quad (4.6)$$

and then substituted along with Equation 4.5 into the governing equation, Equation 3.2, where  $M$ ,  $G$ , and  $K$  are the system mass, damping, and stiffness matrices, respectively,  $F$  is the spatial loading matrix, and  $u$  is the input. This substitution yields

$$[a_0M + a_1G + K]x_{n+1} = Fu + M[a_0x_n + a_2\dot{x}_n + a_3\ddot{x}_n] + G[a_1x_n + a_4\dot{x}_n + a_5\ddot{x}_n] \quad (4.7)$$

where  $a_0$  to  $a_5$  are coefficients that are functions of  $\alpha$ ,  $\delta$ , and  $\Delta t$ . Equation 4.7 is used to solve for the displacements at future time  $t_{n+1}$  using the displacements, velocities, and accelerations at current time  $t_n$ . The velocities and accelerations at  $t_{n+1}$  are then computed using Equations 4.5 and 4.6. The values computed for  $x$ ,  $\dot{x}$ , and  $\ddot{x}$  at  $t_{n+1}$  become  $x$ ,  $\dot{x}$ , and  $\ddot{x}$  at  $t_n$  for the solution at the next time step.

Although Equation 4.7 can be implemented using a *for-loop*; doing so would require the inversion of  $[a_0M + a_1G + K]$  to solve for  $x_{n+1}$ . Because  $M$ ,  $G$ , and  $K$  are typically large, sparse matrices, this does not provide a computationally efficient

solution. However, by transforming  $M$ ,  $G$ ,  $K$ , and  $F$  from a Cartesian coordinate system to a modal coordinate system,  $M$  becomes the identity matrix and  $G$  and  $K$  become diagonal matrices that can then be treated as vectors. This conversion vectorizes Equation 4.7, which can greatly reduce the computational time required once implemented. This kind of approach is a necessity when dealing with real systems that typically have DOFs on the order of tens of thousands.

Damage was simulated by changing local properties such as mass or modulus of elasticity of the model in Figure 4.2. Models can be created for various severity of damage. This is a convenient way of handling damage since it captures the gross effect of damage but doesn't include some non-linear effects such as a crack opening and closing. Including the non-linearities greatly increases the complexity and run time of the simulations without changing the basic outputs of the DMS.

Once the undamaged and damaged models were created, the simulation was run simulating ten seconds of time using a sine chirp function as the input. A time step of 1E-8 was used to ensure smoothness of the input signal. A zero mean random Gaussian noise was added to the input and output measurements with a signal-to-noise ratio (SNR) of 96 dB and 48 dB, respectively. The simulation was run ten times in an undamaged state in order to quantify the statistics of the baseline state and then ten times in a damaged state. Figure 4.10 shows the performance of three optimal designs selected from the Pareto set and three heuristically designed groups. When the damage was introduced at measurement ten, most of the sensor groups responded to the change, and the optimal groups responded in orders of magnitude

greater than the heuristic groups. The same simulations were done for the landing gear with the results shown in Figure 4.11. The simulations were then repeated with the damage in different areas of the part to gauge the overall performance. In these cases the optimal designs consistently outperformed the heuristic ones. Using these simulations an optimal design was chosen for implementation on each component based on its average performance at the hotspot and random locations.

#### **4.3.1.1 Detector Design**

In determining whether or not damage is present a non-subjective method needed to be implemented. Such a method would ideally differentiate between ‘normal’ undamaged behavior and damage behavior. This would be essentially asking the question, “Is there damage in the part under test?” Applying such a method would output a False (zero) or True (one), instead of the continuous damage metric. A standard way to answer this question is via statistical hypothesis testing.

Statistical hypothesis testing is a method of decision-making using experimental data. This process requires stating the null and alternative hypotheses to be tested and considering the statistical assumptions being made about the experimental data. Then, an appropriate statistical test and test statistic can be selected. The distribution of the test statistic under the null hypothesis will typically follow a well-known distribution. Knowing the distribution of the test statistic allows for setting a threshold or significance level that divides the decision space into two regions: acceptance or rejection of the null hypothesis. In this case, a decision criteria is arrived at by

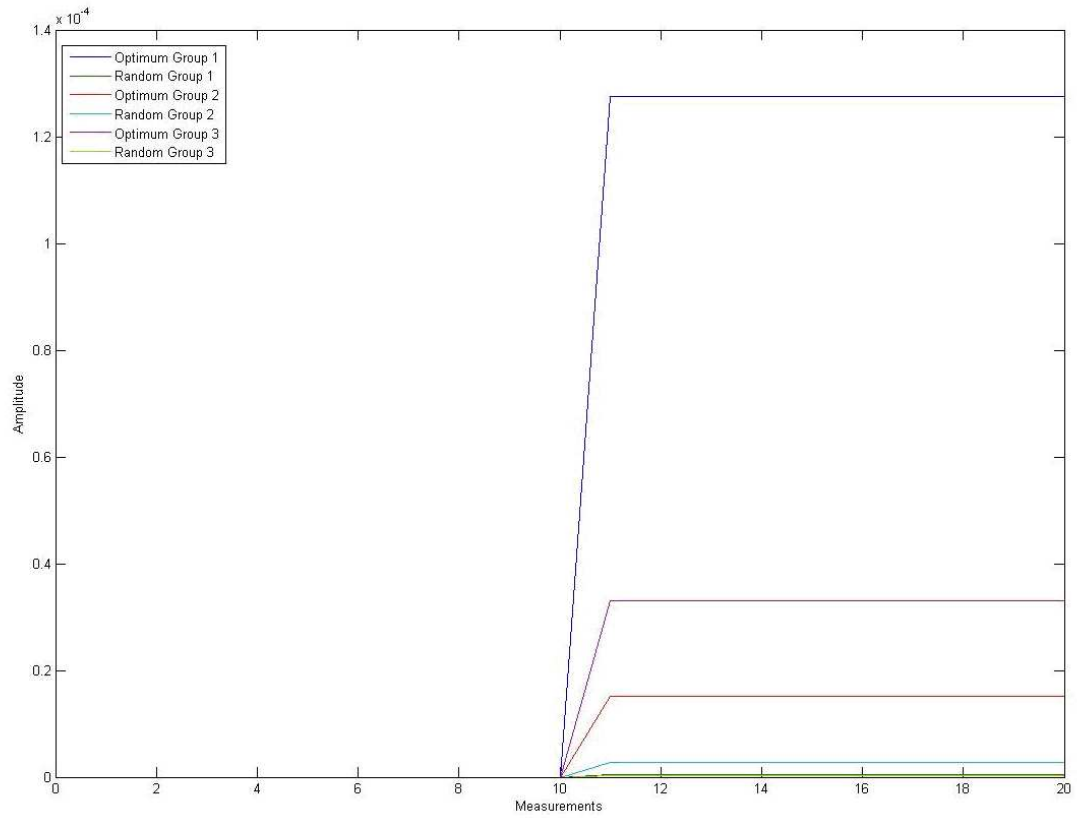


Figure 4.10

Simulated Response of Roof Strap

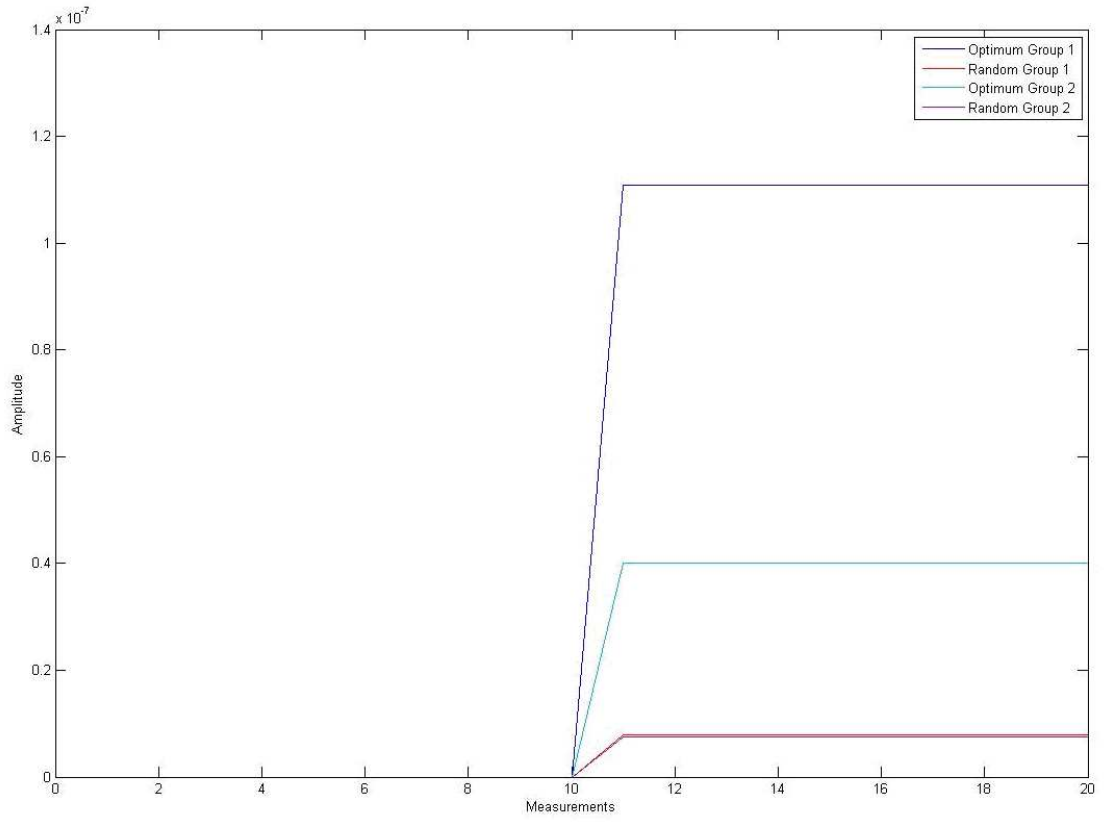


Figure 4.11

Simulated Response of Landing Gear



computing the test statistic using a sample of experimental data. The null hypothesis is rejected if the computed value falls in the critical region or otherwise fails to be rejected.

In applying statistical hypothesis testing to determine if the surrogate is damaged, the surrogate is considered to be undamaged unless there is statistically significant evidence otherwise. The damage metric from the baseline and damage testing phases are assumed to follow a Gaussian distribution. This may not always line up with real data but is a useful assumption nevertheless. With this assumption, an appropriate statistical test is the Z-test. The test statistic,  $Z$ , follows a distribution under the null hypothesis that can be approximated by a normal distribution and is calculated as

$$Z = \frac{\bar{X} - \mu}{\sigma/\sqrt{N}} \quad (4.8)$$

where  $\mu$  and  $\sigma$  are the baseline mean and standard deviation,  $\bar{X}$  is the sample mean, and  $N$  is the sample size. The Z-test tests the null hypothesis that a sample of data is from a normal distribution with known mean and standard deviation against the alternative that the sample mean is not from the known distribution. To establish the undamaged case, a subset of the damage metric baseline data is taken to be a normal distribution from which the known mean and standard deviation for which the null hypothesis are computed. The sample being tested is set of damage metric values from either the baseline and/or damage phase data. Setting the significance level,  $\alpha$ , allows the result to be known with a  $(1 - \alpha)$  confidence level. The Z-test

failing to reject the null hypothesis is interpreted as meaning that the sample is from the baseline distribution and the surrogate is undamaged. The Z-test rejecting the null hypothesis is interpreted as the sample is not from the baseline distribution and the surrogate is damaged.

#### 4.4 Experimental Results

The designs from both the GA and human were then implemented on a landing gear surrogate as shown in Figure 4.12. The piezo was actuated using a sine chirp function ranging from 500 Hz to 8 kHz. The experiment was done where all sensors were simultaneously sampled at 32768 samples per second. In each case, multiple readings from the undamaged or baseline state were taken to establish the statistics of a healthy part. Further measurements were then taken and compared to the baseline state to judge the system's sensitivity to different types of damage. The damage in the landing gear case was simulated by placing a magnet that was 0.01% of the total mass on the structure and then removed. The use of magnets was chosen because the magnets create a change in mass of a structure (simulating corrosion), while allowing the structure to remain physically unaltered. As predicted in simulations, the two optimal sensors outperformed the four heuristic sensors in the majority of cases. As Figure 4.13 shows, the optimal design created by the GA is roughly six times more sensitive than the human-designed one and it uses half as many sensors.

The roof-strap experiment was set up in the same way as the landing gear, with the exception that the frequency range of the sine chirp was extended to 10 kHz.

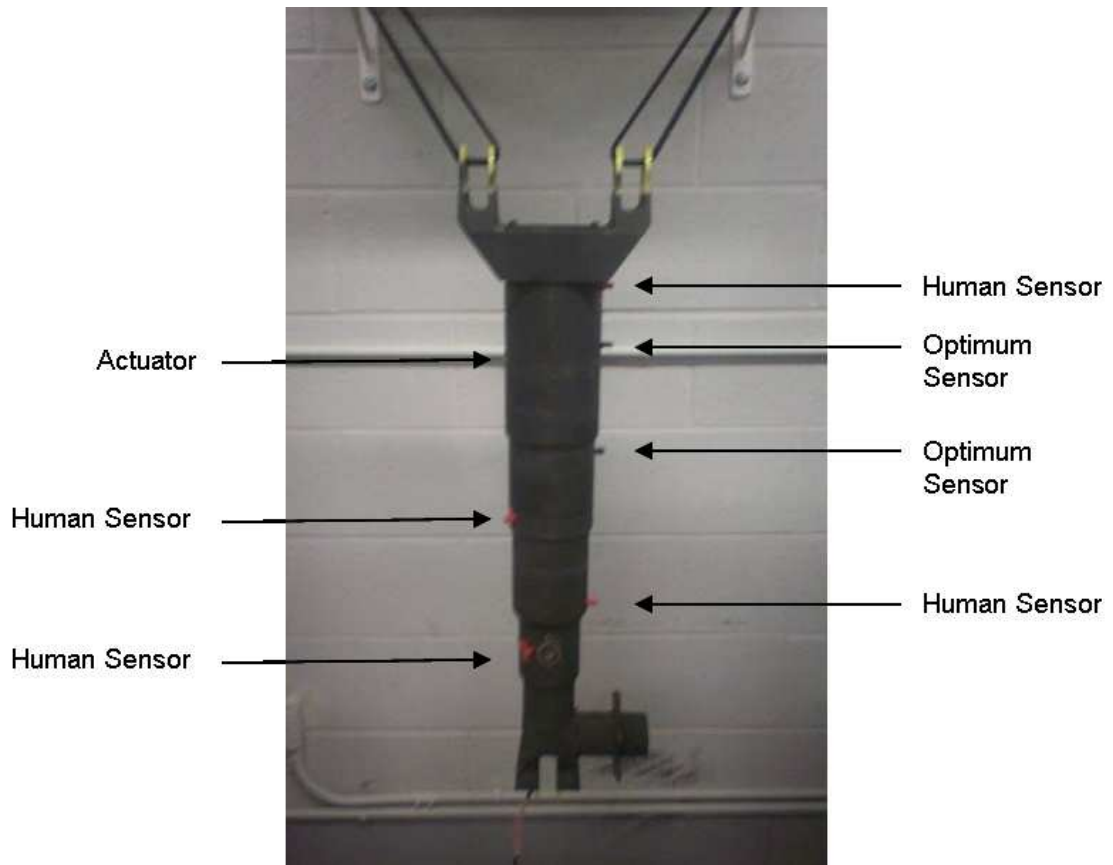


Figure 4.12

Landing Gear Experimental Setup

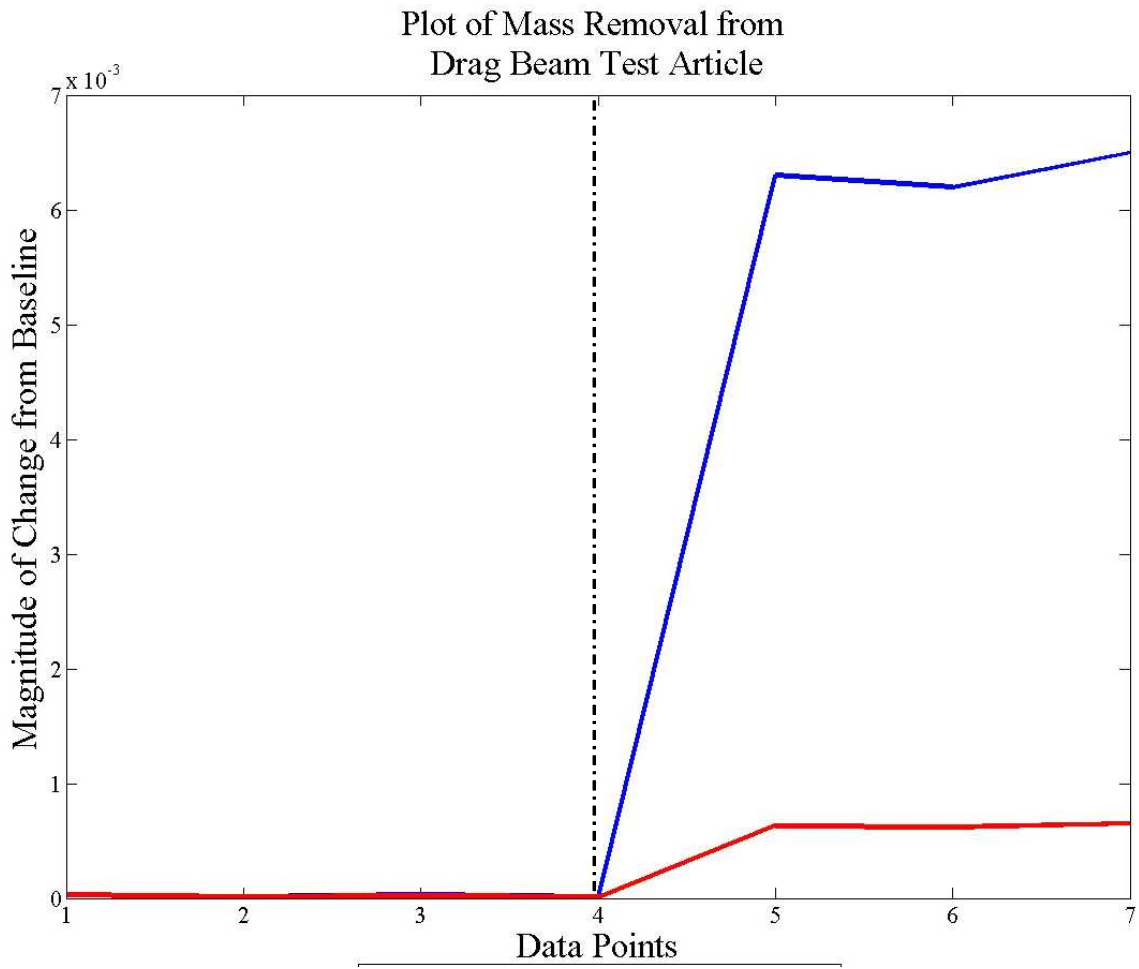


Figure 4.13

Landing Gear Results: Optimal (Blue) Human (Red)

The experimental setup can be seen in Figure 4.14. In this experiment, two different damage cases were simulated. The first damage case was a random bolt (shown in orange) being loosened by 10 in-lbs., then to where it was finger-tight, and finally back to the original tightness. The results of this are shown in Figure 4.15. It was demonstrated yet again that the optimal design is about six times more sensitive than the human-designed one even though it only uses half the number of sensors. In the second damage case, a cut was made in the part to simulate cracking at the location that was identified as the expected damage location from field reports. After the baseline data was collected, a 0.05 in. cut was introduced, then the cut was increased to 0.10 in., 0.15 in., and 0.25 in. The results are shown in Figure 4.16. In the case of monitoring damage where the system was expecting it, the computer implementation was an order of magnitude better than the humans.

The wing attachment fitting experiment was set up similar to the landing gear experiment except that an expected damage location was defined and there would be a range of environmental variable that would affect the boundary conditions of the structure. The health monitoring system was attached and consisted of a piezoelectric actuator and four stud-mounted accelerometers. The test began by collecting a baseline data set. The health monitoring system was then activated ten consecutive times and accelerometer data was collected to measure the undamaged surrogate's response. The surrogate was subjected to increasing amounts of damage with a profile similar to an actual fatigue crack. as introduced by a thin saw blade. The

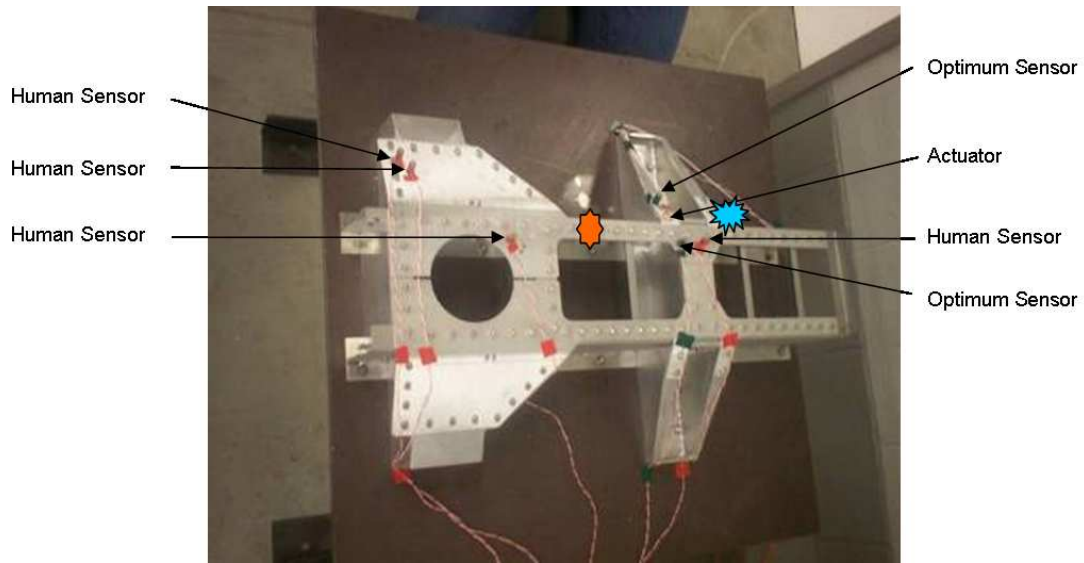


Figure 4.14

### Roof Strap Experimental Setup

cut lengths can be seen in Table 4.1, while a picture of the crack profile is shown in Figure 4.17.

Figure 4.18 plots the damage metric versus the health monitoring system run number with the crack size overlaid. The variations shown in the plot are due to large temperature fluctuations the part was experiencing during testing. Given these fluctuations, the Z-test was implemented using a sliding window of 100 points across the data to determine if the part was damaged. The section shown as “baseline” in Figure 4.18 was used to determine the mean and standard deviation of the damage metric in the undamaged state. The Z-test was then run against the reserved validation data and all data collected after that. The results are plotted in Figure 4.18. The damage metric values from runs 1 to 100 are taken as the first window to be

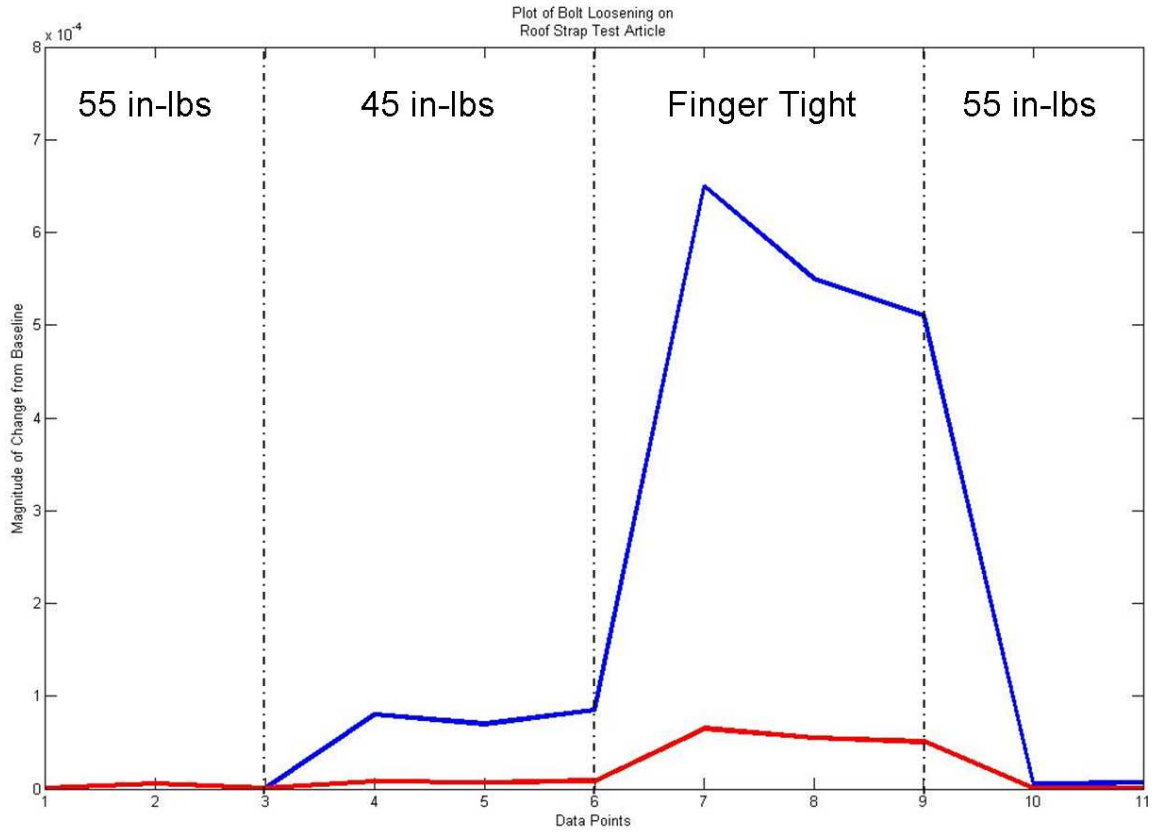


Figure 4.15

Bolt Loosening Results: Optimal (Blue) Human (Red)

Table 4.1

Crack Size & Health Monitoring System Run Numbers

Cut #	Crack Size (in)	Run Numbers	Cut #	Crack Size (in)	Run Numbers
0	0.0 (Baseline)	1-1141	8	0.248	2822-3061
1	0.020	1142-1381	9	0.297	3062-3301
2	0.040	1382-1621	10	0.401	3302-3541
3	0.064	1622-1861	11	0.498	3542-3781
4	0.082	1862-2101	12	1.000	3782-4021
5	0.096	2102-2341	13	1.504	4022-4261
6	0.149	2342-2581	14	2.002	4262-4501
7	0.202	2582-2821			

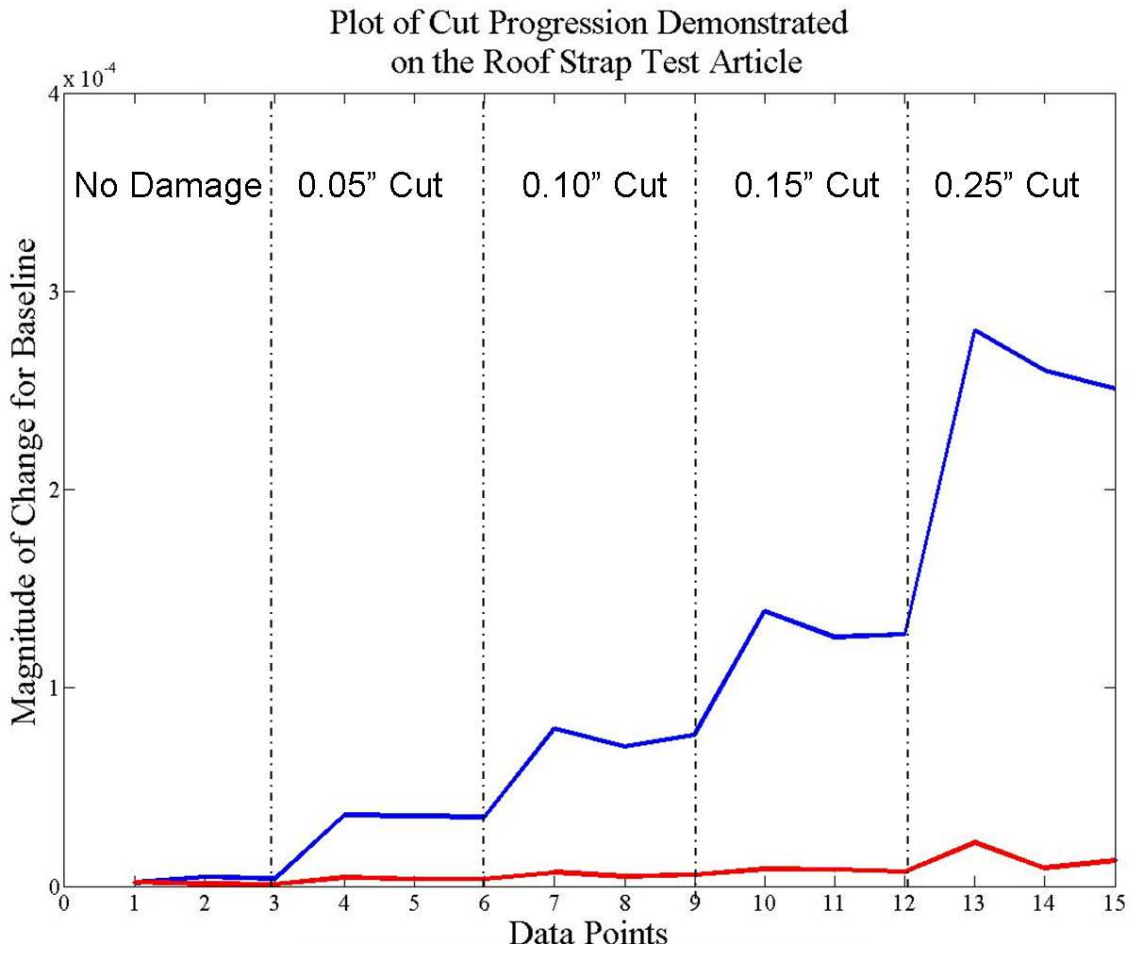


Figure 4.16

Roof Strap Cut Results: Optimal (Blue) Human (Red)



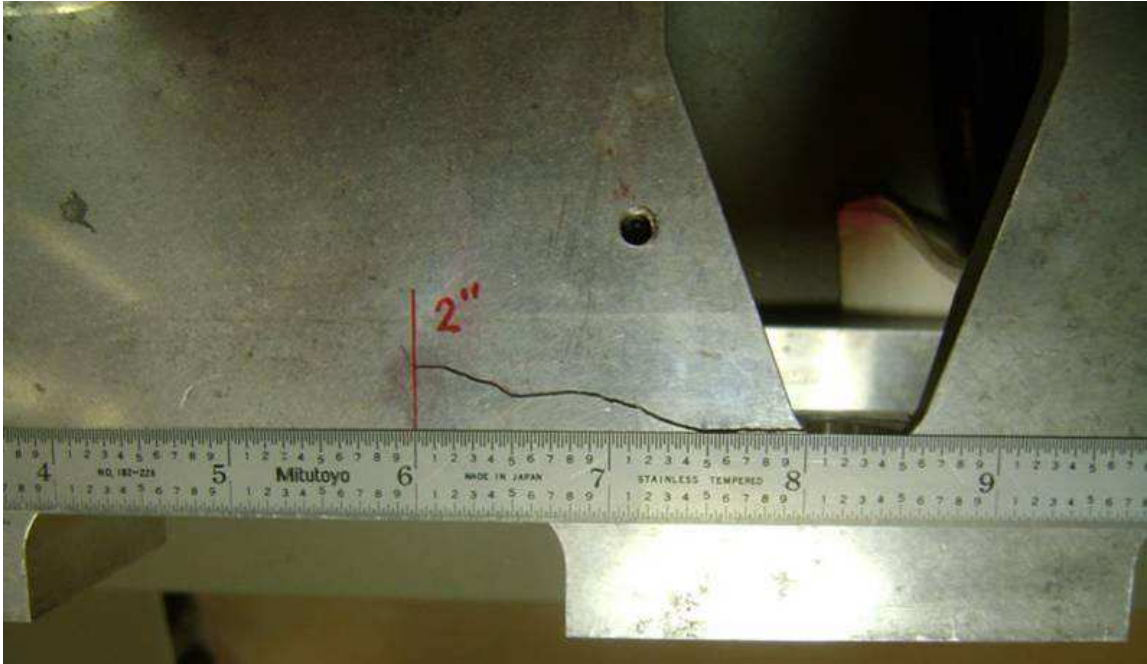


Figure 4.17

Cut at Completion of Test

used in the Z-test, next values from runs 2 to 101 are used, followed by values from runs 3 to 102, and so on. The outcome of the test is either zero or one and is plotted in Figure 4.19. A zero indicates a failure to reject the null hypothesis, implying the surrogate is undamaged, whereas a one indicates a rejection of the null hypothesis, implying the surrogate is damaged. The Z-test is applied at a  $10^{-6}\%$  significance level, providing a 99.999999% confidence level in the test result. Some things to note are that there are no false positives (i.e., indications that the surrogate is damaged when it is not damaged), and at eleven points into the damage phase data, this optimal design was able to indicate with 99.999999% confidence that the surrogate was damaged. The false negatives (i.e., indicating the surrogate was not damaged

when it was damaged) only occurred when the crack size was 0.04 inches or less. One way to evaluate the performance of the detector is to formulate a confusion matrix that gives the rate of hits and misses. A confusion matrix is a table with two rows and two columns that reports the true positive, false positive, false negative, and true negative detection rates. The confusion matrices for the damage metric data is presented in Table 4.2.

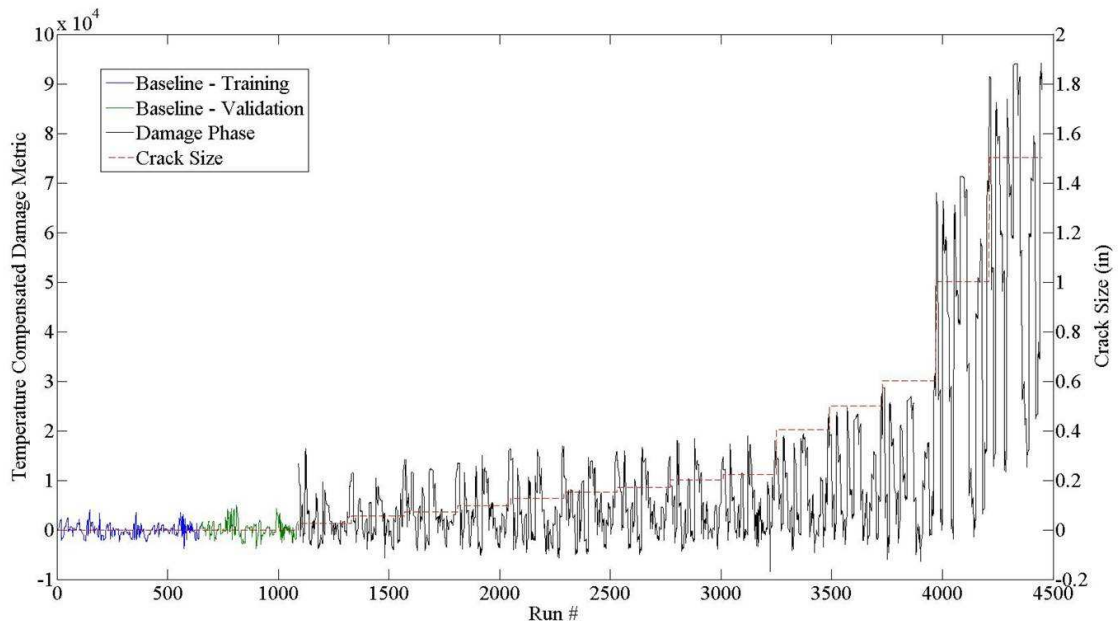


Figure 4.18

Damage Metric vs. Sample Number with Crack Size Overlaid

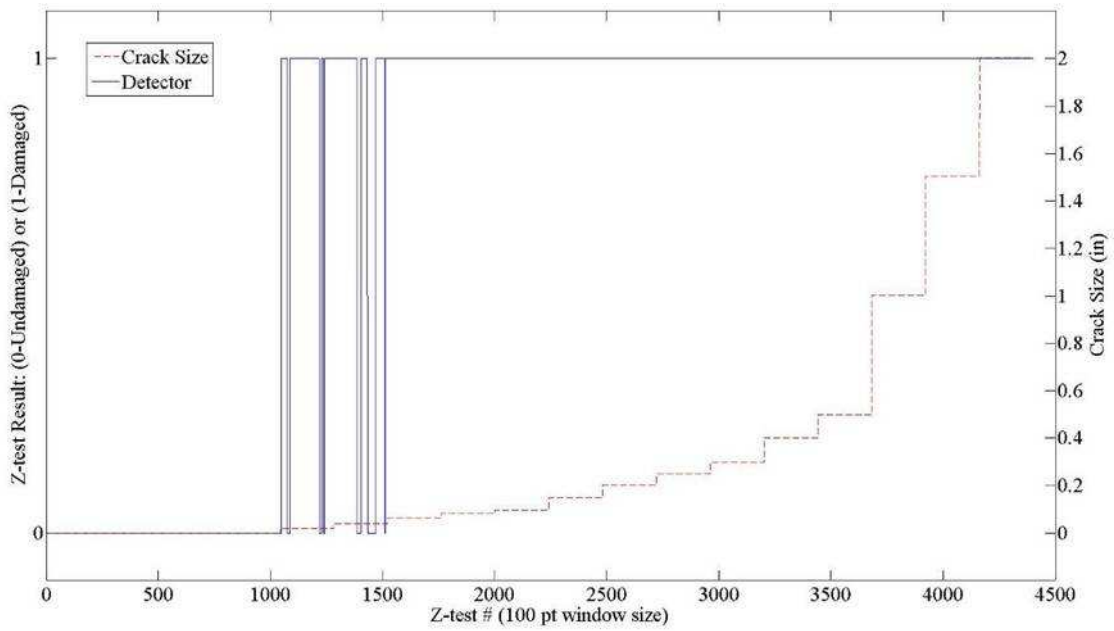


Figure 4.19

Z-Test Result at 99.999999% Confidence; Crack Size Overlaid

Table 4.2

Confusion Matrix for Statistical Damage Detector

True Negatives	False Positives
100.0%	0.0%
False Negatives	True Positives
8.2%	91.8%

## CHAPTER 5

### CONCLUSIONS

#### 5.1 Summary of Work

This dissertation examined a systematic method for designing sensor and actuator systems for structural health monitoring. As engineers and fleet managers have to do more with fewer resources, causing structures to be used well past their intended lifetime, SHM has become an area of interest with potential of extending the safe life usage in aerospace, civil, and mechanical structures. This work began with an introduction to the topic of health monitoring including motivational drivers and basic concepts. Work conducted by various researchers was reviewed but most of the existing knowledge lay in the areas of transducer technology, modeling, signal processing, and pattern classification. A clear need for a systematic method to bring all these disparate pieces together into a single framework that allows for the balancing of various design needs was shown.

In this work such a framework was developed. The framework is based on optimal design principles and concepts from System Theory. It allows for a formal methodology using parametric models and mathematical metrics for design evaluation that is flexible enough to handle multiple simultaneous design objectives. The results of a design is a set of possible sensor and actuator locations that are spread

out over the Pareto surface representing all optimal trade-offs in the solution space. This allows a designer to visualize all the possibilities and find a solution that meet their criteria. Having a set of optimal trade-offs is also beneficial if design priorities change, as it allows a new solution to be picked without rerunning the optimization, which is by far the most time consuming part of a design, and it is especially useful when the structure is designed concurrently with the monitoring system, as it allows for different design choices to be made that can greatly impact the overall system performance.

In addition to the design framework, some specific objective functions for health monitoring systems were developed. These included objective functions for:

- optimizing sensor and actuator positions and type for detecting damage in expected locations (hotspots);
- optimizing sensor and actuator positions and type for detecting damage globally; and
- being robust to modeling error and manufacturing variations.

The optimal sensor and actuator positioning for hotspot objective was derived from the standard implementation of the controllability grammian and the global damage detection objective was extended from the observability grammian. The robustness to modeling error and manufacturing variations was developed by formalizing the sensitivity of a particular design to the parameters used in creating the model upon which that the design was based.

The design framework and the objective functions were then brought together to create health monitoring systems for three different structures: a landing gear, roof

strap, and wing fitting. Because of the topology of the problem, the scheme chosen to perform the optimization was a genetic algorithm; though it should be noted, it is not the only choice of acceptable optimization method. After the optimization was performed, the designs selected were then simulated under various assumptions to evaluate the effectiveness of the objective functions. It was shown that the design was sensitive to damage occurring in both an expected and unexpected location by first comparing the optimization results to an exhaustive search using a highly simplified model and, second, by fixing some design variables and then performing a quasi-exhaustive search on a more complex structure with many local minima in the search space. The results showed that the designs were maximally sensitive in locations that the algorithm was told damage should be expected to be found, while at the same time it showed acceptable levels of sensitivity at all other locations in the structure. The design robustness objective was analyzed by numerically estimating the sensitivities to the model and by Monte Carlo analysis, which involved simulating the design performance over a range of possible models. In the numerical case, the sensitivity was estimated using Newton's difference quotient. This sensitivity was then shown, in the context of real-world performance, to be such that for all modern modeling and manufacturing techniques that the system performance lost due to errors would be below any realistic electronic noise floor. In other words, because of the objective function, the optimization chose solutions that were highly insensitive to the parameters of the underlying model and real world performance would not be adversely affected by modeling error and manufacturing variations. This analysis was

confirmed by the Monte Carlo simulations, which showed that the designs produced using the objective functions tended to produce the same answer using a model with a wide range of physical parameters and boundary conditions.

With the objective functions effectiveness verified under simulated results, the designs were implemented on real aerospace structures. On each structure a baseline was defined to quantify the statistical behavior of the damage metric while in an undamaged state. Once the statistics were known, a detector was implemented using a Z-Test to determine if damage was present in the structure under test. First the results of mass changes, which are representative of pitting, were shown on a landing gear. The system, which was designed using only the global damage metric, was sensitive enough to detect a mass change that was less than 0.01% of the total mass of the structure. Next, results of a bolt loosening and crack growing on a roof strap were shown and then comparisons were made to a health monitoring system designed by expert knowledge. The results showed the optimally designed system could readily detect the bolt loosening at an unexpected location and was sensitive enough to detect a 0.05 in. flaw. In all cases the optimal system was shown to out perform the expert system even though it used only half the number of sensors. Finally, the results of the wing attachment experiment showed that, with proper system and detector design, damage as small as 0.02 in. can be detected with a high confidence even with fluctuations in the boundary conditions.

While the methods demonstrated in this work used only accelerometers, it (and similar methods), apply to a much broader set of sensing technologies. With these

methods, structural health monitoring systems can be designed using any combination of strain, vibration, thermal, or electromagnetic sensors with the purpose of having maximum sensitivity to damage occurring in known or unknown locations on a structure.

## 5.2 Recommendation for Continued Research

There are still several issues worthy of consideration to further advance the field of structural health monitoring. One major issue that isn't being discussed in depth at this time, is the concept of "what is damage" and "when is a structure considered 'not healthy'?" A good number of the researchers in this field are from a non-destructive inspection (NDI) background. In the field of NDI, since the plane is already out for maintenance, the focus is trying to characterize very small flaws since the next inspection interval may be large and this mentality has carried over to health monitoring. It is this author's feeling that health monitoring has a different goal than NDI. Health monitoring is more of a continuous process that alerts the maintenance crews of structural weaknesses that make the vehicle unsafe to operate. This is similar to having a virus in your body; one single virus may not be that bad for your health but many of that kind can cause the flu. Similarly, a single small crack may not pose a risk to a air vehicle but many small ones can be extremely risky. Using these analogies, many people are trying to approach health monitoring like NDI where very small flaws are found even if they pose no risk to the structure. Under a SHM paradigm, where inspections can be run daily, the question should be framed



as “how fit is this structure to perform its designed mission?” and “if it is damaged can it operate in a reduced capacity?” One possible way to answer these questions is using the FE models developed for sensor placement and damage detection and then perform studies to see how much the operational load is reduced given certain amounts of data. This approach means that, once your health monitoring system told you how much damage is present in a certain area, one could truly assess the risk to the vehicle.

Other areas worth future consideration include developing additional objective functions to fit into the presented framework. Some possible functions are competing different signal processing methods or, objectives for the ability to localize the damage and characterize the extent of damage. Since the signal processing method proposed herein has no claim to being optimal, all though it has proven to be effective in a variety of cases, there is the possibility that alternative signal processing methods can improve performance or even that there are a multitude of methods that should be selected based on the application. In these cases, competing the signal processing methods in addition to the types and location of sensors could be of great benefit. This effort made no attempt to localize and characterize the amount of damage in the structure even though there is evidence of a correlation between the damage metric and the extent of damage. Knowing the location and extent of damage has obvious advantage to the prediction of remaining life in a structure. As such, work should be done in defining methods to reliably locate and estimate the amount of damage in a component. A traditional barrier to localizing damage is that either one has

to use high frequency pulse-echo signal, a concept similar to radar in the structure which has limited global usage due to the number of scatterers (bolts, ribs, etc.) in a realistic part, or have highly accurate models, which is typically beyond current modeling capabilities for complex structures, that allow for a model-inversion type of solution. Serious attempts to address these limitations is the concept of damage location vectors [10]. Once any single technique shows promise in addressing these problems, a formalized metric on how to design systems to enhance its performance should be derived and incorporated into the presented framework.

One other area ripe for exploration is to optimally design the excitation signal. In this work the excitation signal was a sine chirp, which allowed all modes and areas of the structure to be excited equally. The ability to selectively excite one area versus another would be a benefit to any localization efforts and judicious design of an input signal could improve additional areas of performance, such as damage detection. It is anticipated that using some concepts from dynamic optimization, such as optimal trajectories, an interrogation signal could be designed, in a similar manner presented here, for the purpose of maximizing or minimizing the same objective functions as used in the sensor and actuator designs. This would allow another degree of flexibility in achieving robust results.

## BIBLIOGRAPHY

- [1] J. S. Bendat and A. G. Piersol, *Engineering Applications of Correlation and Spectral Analysis, 2nd Edition*, 2 edition, Wiley-Interscience, Feb. 1993.
- [2] R. Brown and H. Willis, “The economics of aging infrastructure,” *Power and Energy Magazine, IEEE*, vol. 4, no. 3, 2006, pp. 36–43.
- [3] A. E. Bryson, *Dynamic optimization*, Addison Wesley Longman, 1999.
- [4] E. Carden and P. Fanning, “Vibration based condition monitoring: a review,” *Structural Health Monitoring*, vol. 3, no. 4, 2004, p. 355.
- [5] P. Chang, A. Flatau, and S. Liu, “Review paper: health monitoring of civil infrastructure,” *Structural Health Monitoring*, vol. 2, no. 3, 2003, p. 257.
- [6] A. Cherng, “Optimal sensor placement for modal parameter identification using signal subspace correlation techniques,” *Mechanical Systems and Signal Processing*, vol. 17, no. 2, 2003, pp. 361–378.
- [7] R. Cobb and B. Liebst, “Sensor placement and structural damage identification from minimal sensor information,” *AIAA journal*, vol. 35, no. 2, 1997, pp. 369–374.
- [8] K. Deb and H. Gupta, “Searching for robust Pareto-optimal solutions in multi-objective optimization,” *Evolutionary Multi-Criterion Optimization*. Springer, 2005, pp. 150–164.
- [9] K. Dhuri and P. Seshu, “Multi-objective optimization of piezo actuator placement and sizing using genetic algorithm.,” *Journal of Sound & Vibration*, vol. 323, no. 3-5, 2009, pp. 495 – 514.
- [10] M. Dionisio Bernal, “Load vectors for damage localization,” *Journal of Engineering Mechanics*, vol. 128, 2002, p. 7.
- [11] S. Doebling, C. Farrar, M. Prime, and D. Shevitz, *Damage identification and health monitoring of structural and mechanical systems from changes in their vibration characteristics: a literature review*, Tech. Rep. LA–13070-MS, Los Alamos National Lab., NM (United States), 1996.
- [12] R. Fletcher, *Practical Methods of Optimization*, 2nd edition, Wiley, May 2000.

- [13] C. Fonseca, P. Fleming, et al., “Genetic algorithms for multiobjective optimization: Formulation, discussion and generalization,” *Proceedings of the fifth international conference on genetic algorithms*. Citeseer, 1993, pp. 416–423.
- [14] W. Frazier and D. L. Parker, *Nondestructive Evaluation Technology Initiatives, Delivery Order 0035; Dynamical Systems Engineering Research for Structural Integrity Monitoring of Space Systems*, Tech. Rep., AFRL, 2003.
- [15] H. Gao and J. Rose, “Sensor placement optimization in structural health monitoring using genetic and evolutionary algorithms,” *Proceedings of SPIE*, 2006, vol. 6174, p. 617410.
- [16] P. E. Gill, W. Murray, and M. H. Wright, *Practical Optimization*, Academic Press, 1982.
- [17] A. Gramopadhye and C. Drury, “Human Factors in Aviation Maintenance: how we got to where we are,” *International Journal of Industrial Ergonomics*, vol. 26, no. 2, 2000, pp. 125–131.
- [18] H. Guo, L. Zhang, L. Zhang, and J. Zhou, “Optimal placement of sensors for structural health monitoring using improved genetic algorithms,” *Smart Materials and Structures*, vol. 13, 2004, pp. 528–534.
- [19] M. Haftka Howard and T. Raphael, “Selection of actuator locations for static shape control of large space structures by heuristic integer programming,” *Computers & Structures*, vol. 20, no. 1-3, 1985, pp. 575–582.
- [20] H. Hochman and J. Rodgers, “Pareto optimal redistribution,” *The American Economic Review*, vol. 59, no. 4, 1969, pp. 542–557.
- [21] A. Jardine, D. Lin, and D. Banjevic, “A review on machinery diagnostics and prognostics implementing condition-based maintenance,” *Mechanical systems and signal processing*, vol. 20, no. 7, 2006, pp. 1483–1510.
- [22] T. Kailath, *Linear systems*, Prentice-Hall Englewood Cliffs, NJ, 1980.
- [23] D. Kammer, “Sensor placement for on-orbit modal identification and correlation of large space structures,” *Journal of Guidance, Control, and Dynamics*, vol. 14, no. 2, 1991, pp. 251–259.
- [24] S. Kim, S. Pakzad, D. Culler, J. Demmel, G. Fenves, S. Glaser, and M. Turon, “Health monitoring of civil infrastructures using wireless sensor networks,” *Proceedings of the 6th international conference on Information processing in sensor networks*. ACM, 2007, p. 263.
- [25] R. Kincaid and S. Padula, “D-optimal designs for sensor and actuator locations,” *Computers & Operations Research*, vol. 29, no. 6, 2002, pp. 701–713.

- [26] K. Laermann, “Assessment of structural integrity and durability– a task of experimental mechanics,” *Meccanica*, vol. 45, no. 2, 2010, pp. 167–174.
- [27] J. Lin, “Multiple-objective problems: Pareto-optimal solutions by method of proper equality constraints,” *Automatic Control, IEEE Transactions on*, vol. 21, no. 5, 2002, pp. 641–650.
- [28] C. Papadimitriou, “Optimal sensor placement methodology for parametric identification of structural systems,” *Journal of Sound and Vibration*, vol. 278, no. 4-5, 2004, pp. 923 – 947.
- [29] V. Pareto, *Manual of political economy*, Augustus m Kelley Pubs, 1971.
- [30] C. Phillips and R. Habor, *Feedback control systems*, Simon & Schuster, 1995.
- [31] A. Raich and T. Liskai, “Multi-objective genetic algorithm methodology for optimizing sensor layouts to enhance structural damage identification,” *Proc. of the 4th Intational Workshop on Structural Health Monitoring*, F.-K. Chang, ed. 2003, DEStech Publications, Inc.
- [32] J. Reason and A. Hobbs, *Managing maintenance error: a practical guide*, Ashgate Publishing, 2003.
- [33] H. Rinehart, *Model Based Optimal Design for Structural Health Monitoring*, master’s thesis, University of Mississippi, 2005.
- [34] N. Roy and R. Ganguli, “Filter design using radial basis function neural network and genetic algorithm for improved operational health monitoring,” *Applied Soft Computing*, vol. 6, no. 2, 2006, pp. 154 – 169.
- [35] A. Rytter, *Vibration Based Inspection of Civil Engineering Structures PhD Dissertation*, doctoral dissertation, Department of Building Technology and Structural Engineering, Aalborg University, Denmark, 1993.
- [36] C. Sekine-Pettite, “Structural Health Monitoring,” *Bridges*, vol. 8, no. 2, 2005.
- [37] Z. Shi, S. Law, and L. Zhang, “Optimum Sensor Placement for StructuralDamage Detection,” *Journal of Engineering Mechanics*, vol. 126, 2000, p. 1173.
- [38] R. Skelton and M. DeLorenzo, “Selection of noisy actuators and sensors in linear stochastic systems,” *Journal of Large Scale Systems, Theory and Applications*, vol. 4, 1981, pp. 109–136.
- [39] C. Swann and A. Chattopadhyay, “A Stochastic Approach to Optimum Sensor Placement for Damage Detection,” *Proc. of the 5th Intational Workshop on Structural Health Monitoring*, F. Chang, ed. 2005, DEStech Publications, Inc.

- [40] H. Yaiche, R. Mazumdar, and C. Rosenberg, “A game theoretic framework for bandwidth allocation and pricing in broadband networks,” *IEEE/ACM Transactions on Networking (TON)*, vol. 8, no. 5, 2000, pp. 667–678.
- [41] Y. Yan, H. Chen, and J. Jiang, “Optimal placement of sensors for damage characterization using genetic algorithms,” *Key Engineering Materials*, vol. 334, no. 2, 2007, p. 1033.
- [42] K. Yuen, L. Katafygiotis, C. Papadimitriou, and N. Mickleborough, “Optimal sensor placement methodology for identification with unmeasured excitation,” *Journal of Dynamic Systems, Measurement, and Control*, vol. 123, 2001, p. 677.
- [43] E. Zitzler and L. Thiele, “Multiobjective optimization using evolutionary algorithms—a comparative case study,” *Parallel Problem Solving from Nature*. Springer, 1998, p. 292.